HELSINKI UNIVERSITY OF TECHNOLOGY

Faculty of Electronics, Communications and Automation

Anna-Sofia Kiveliö

Superhydrophobic Coating for Reducing Unwanted Cell and Bacterial Adhesion in Medical Implants

Diplomityö, joka on jätetty opinnäytteenä tarkastettavaksi diplomi-insinöörin tutkintoa varten Espoossa 5.11.2009

Työn valvoja Professori Mervi Paulasto-Kröckel

Työn ohjaaja Markus Turunen, C. P. Wong, Barbara Boyan

November 13, 2009

TEKNILLINEN KORKEAKOULU **Diplomityön tiivistelmä**

Tekijä: Anna-Sofia Kiveliö

Työn nimi: Superhydrophobic Coating for Reducing Unwanted Cell and Bacterial Adhesion in Medical Implants

Sivumäärä: 83

Päivämäärä: 5.11.2009

Tiedekunta: Elektroniikka, tietoliikenne ja automaatio

Professuuri: S-113, Elektroniikan valmistustekniikka

Työn valvoja: Mervi Paulasto-Kröckel

Työn ohjaajat: Markus Turunen, C. P. Wong ja Barbara Boyan

TYÖN TARKOITUS: Tämän diplomityön tarkoituksena oli valmistaa ja karakterisoida superhydrofobinen pinnoite sekä arvioida solujen ja bakteerien vastetta tälle pinnoitteelle, perustuen hypoteesiin, jonka mukaan superhydrofobinen pinnoite vähentää bioadheesiota tai estää sen täysin.

MATERIAALIT JA MENETELMÄT: Lasi- ja titaanikiekkoja päällystettiin superhydrofobisella pinnoitteella, sekä kahdella pinnoitteella (mikro- ja nanokonstruoitu pinnoite ja matalan pintaenergian pinnoite), joista superhydrofobinen pinnoite koostuu. Alkuperäisestä pinnoitteesta valmistettiin myös polydimetyylisiloksaani (PDMS) polymeeriä sisältävä muunnos, minkä tarkoituksena oli parantaa pinnoitteen mekaanisia ominaisuuksia mahdollista pehmeiden materiaalien päällystämistä varten. Solujen vastetta pinnalle testattiin 1. viljelemällä soluja pinnoilla ja tarkastelemalla kiinnittyneiden solujen määrää ja ulkomuotoa 2. MTT testillä, jolla voidaan arvioida biomateriaalien solumyrkyllisyyttä.

TULOKSET: Superhydrofobinen pinnoite vähensi solujen ja bakteerien adheesiota huomattavasti, sekä kontrollinäytteisiin, että yksittäisiin pinnoitteisiin verrattuna. Minkään pinnoitteista, PDMS muunnos mukaan lukien, ei havaittu olevan soluille myrkyllinen.

YHTEENVETO: Näiden alustavien tulosten perusteella voidaan sanoa, että tämä superhydrofobinen pinnoite soveltuu käytettäväksi sellaisten implanttien päällystämiseen, joihin solujen ja bakteerien adheesio ei ole toivottua.

Avainsanat: Superhydrofobinen, sooli-geeli, likaantumaton pinnoite, soluadheesio

HELSINKI UNIVERSITY OF TECHNOLOGY Abstract of the Master's Thesis

Author: Anna-Sofia Kiveliö

Name of the thesis: Superhydrophobic Coating for Reducing Unwanted Cell and Bacterial Adhesion in Medical Implants

Number of pages: 83

Date: 5.11.2009

Faculty: Electronics, Communications and Automation

Professorship: S-113, Electronics Production Technology

Supervisor: Mervi Paulasto-Kröckel

Instructors: Markus Turunen, C. P. Wong and Barbara Boyan

PURPOSE: The purpose of this master's thesis was to prepare and characterize superhydrophobic coatings and to evaluate cell and bacterial response to them, based on the hypothesis that superhydrophobic surfaces reduce or completely block bioadhesion.

MATERIALS AND METHODS: Glass and titanium disks were coated with a superhydrophobic coating, consisting of two different coatings (micro- and nanostructured coating and a low surface energy coating), as well as just these two coatings. Modification of the coating with polydimethylsiloxane (PDMS) was also done in order to enhance its mechanical properties for coating softer materials. Cell response was tested by 1. culturing cells on the surfaces and evaluating their attachment by determining the number cells as well as examining cell morphology 2. MTT cell viability assay to evaluate coating toxicity.

RESULTS: Superhydrophobic surfaces displayed considerably reduced cell and bacterial adhesion compared to control samples, as well as the two individual coatings making up the superhydrophobic coating. No evidence of coating toxicity of the original coating or the PDMS modification was observed.

CONCLUSION: Based on these preliminary tests, superhydrophobic coating can be used for coating medical implants in instances where cell and bacterial adhesion is not desired.

Keywords: Superhydrophobic, sol-gel, anti-adhesion coating, cell adhesion

ACKNOWLEDGEMENTS

The research for this master's thesis was carried out during 1.11.2008-1.8.2009 at Georgia Institute of Technology in United States. I would like to thank Dr. C.P. Wong and Dr. Barbara Boyan for the opportunity to join their groups for the duration of my stay, as well as all the other members of their groups for their help in my research.

From TKK I would like to thank Markus Turunen for comments and advise on my thesis, as well as guidance during my studies. I would also like to express my gratitude to professor Jorma Kivilahti for making it possible for me to go to Georgia Tech and professor Mervi Paulasto-Kröckel for supervising my thesis.

Lastly, I want to thank my mom and my dad and friends who supported me during the completion of this project. To my former housemates in Atlanta and all the other new friends I made, it was a great year, thanks y'all.

Espoo 29.10.2009

Anna-Sofia Kiveliö
Säterinkatu 10 B 22
02600 Espoo

Table of Contents

Abbreviations

3T3 cells 3-day transfer, inoculum 3 x 10^5 cells
ACNT Aligned carbon nanotube
AFM Atomic force microscopy
BHK Cells baby hamster kidney cells
C-U Choline chloride – Urea
CBD Chemical bath deposition
CF_4 Tetrafluoromethane
CVD Chemical vapor deposition
DAPI 4',6-diamidino-2-phenylindole
DI-water De-ionized water
DMEM Dulbecco's modified Eagle medium
DMSO Dimethyl sulfoxide
ECM Extracellular matrix
EPS Extracellular polymeric substances
ePTFE Polytetrafluoroethylene
FAS Fluoroalkylsilane
FBS Fetal bovine serum
FEP-Teflon Fluorinated ethylene propylene copolymer teflon
FMOB Full osteoblast media
HCl Hydrochoric acid
HEMAPC Hydroxyethylmethacrylate phosphatidylcholine
HeLa cells Henrietta Lacks cells
HF Hydrofluoric acid
HMM-kininogen High-molecular-mass kininogen
HUVEC Human umbilical vein endothelial cell
LBL Deposition layer-by-layer deposition
LDH Lactate dehydrogenase
LDPE Low density poly(ethylene)
MPECVD Microwave-plasma-enhanced chemical vapor deposition
MTT 3-(4,5-Dimethylthiasol-2-yl)-2,5-diphenyltetrazolium bromide
NaCl Natrium chloride
NaOH Natrium hydroxide
NH_4OH Ammonium hydroxide
ODPA Octadecylphosphonic acid
P123 tri-block copolymer pluronic P123
PBS Phosphate buffered saline
PCU Poly(carbonate urethane)
PDMS Polydimethylsiloxane
PE-CVD Plasma enhanced-chemical vapour deposition
PET Polyethylenetherephtalate

PFOS Perfluorooctyl trichlorosilane
PLLA Poly(L-lactic acid)
PRP Platelet-rich plasma
RF Radio frequency
SAM Self-assembled monolayer
SEM Scanning electron microscopy
SiO_2 Silicon oxide
Ti-A-S Fine polished titanium alloy (Ti-6Al-4V)
TCPS Tissue culture polystyrene
TEOS Tetraethyl-orthosilicate
$Ti0_2$ Titanium oxide
TMOS Tetramethyl-orthosilicate
UV-ozone Ultra violet ozone
VUV Vacuum ultraviolet lithography
XPS X-ray photo electron spectroscopy

1 Introduction

Surface engineering of biomaterials has become more and more focused on texturing surfaces at the micro- to nanoscale in order to control important interfacial events, such as protein adsorption and cell adhesion, crucial for implant performance. One subgroup of these textured materials with different types of surface roughness are poorly water-wettable (hydrophobic) materials displaying superhydrophobicity or ultrahigh water repellency, sometimes also referred to as ultrahydrophobic [1][2] or super anti-wetting [3] in the literature.

Superhydrophobicity, in other words extreme water repellency, was first observed in the leaves of the Lotus plant (Figure 1) [4]. As water comes in contact with the surface of the leaf it forms droplets and rolls off, also taking dirt particles along with it. Detailed inspection of the leaves has shown micron and submicron structures as well as hydrophobic substances on the leaf surface [5], which have since been determined to be the two factors leading to superhydrophobicity. [6] To this day, a multitude of different methods have been developed for fabricating superhydrohobic surfaces from synthetic materials.

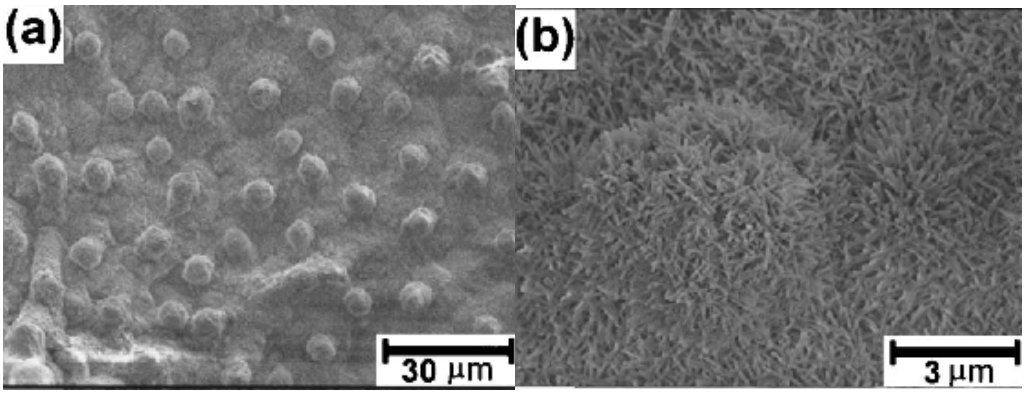

Figure 1 SEM image of Lotus leaf displaying the two scale roughness, composed of microscale bumps and nanoscale hairlike structures [7]

The hydrophobicity of a surface is defined according to the surface energy (surface chemistry) as well as the roughness of the surface. Superhydrophobicity has two requirements: the surface has to have a low surface energy due to the surface chemistry and it has to be micro/nanostructured. [8] Superhydrophobic surfaces have been studied extensively in recent years since they have a large number of potential applications in different fields, e.g. surface decontamination in microelectronics, marine fouling, corrosion prevention, coatings for biomedical devices and friction reduction [3]. They have been

hypothesized to effectively prevent cell adhesion but there has been only a small number of papers published focusing on this area.

The success of implanted devices such as biosensors, orthopedic implants, cardiovascular prosthesis, neural electrodes and drug delivery devices is dependent on the ability to control the behavior of cells that interact with implanted biomaterials. Implant performance is affected by the ability of cells to interact with the exposed device material which often leads to the failure of the implant. For example, adherent macrophages and foreign body giant cells in the foreign body reaction are known to lead to degradation of biomaterials with subsequent clinical device failure [9] and the adhesion of nervous system cells to the lumen of cerebrovascular shunts can lead to their failure by obstruction [10]. Thus materials that can limit the adhesion and viability of cells on implanted biomaterials are needed. [11]

In addition to the inability to control cell adhesion, infection also remains to be a major problem in the long-term performance of many implanted devices. The success of an organism as a pathogen is dependent upon its ability to adhere to the surface and remain there under the protective covering of the extracellular material forming the biofilm. Infections mainly arise from the patient's skin or mucus membrane, the hands of the surgical or the clinical staff during the implantation process, contaminated disinfectants, other patients in the hospital or distant local infections. Most of these infections cannot be controlled with antibiotics and it may become necessary to remove the implanted device from the patient which is of course expensive and poses another threat to patient's health. [12]

Research employing superhydrophobicity in the biomedical area is somewhat scarce, though, in some cases it could be of interest to develop biomaterials preventing the adhesion of cells or tissues at least in some regions. Templating superhydrophobic regions onto the materials surface could be used to pattern cells or to control tissue outgrowth [13]. Possible biomedical applications could be for example membranes for guided tissue regeneration or films with one of the sides is in contact with blood, in which case it might be advantageous for one of the sides of the material to be water repellent, avoiding the linkage with tissues or blood coagulation [14]. Also dental biomaterials [15], implantable shunt and catheter systems [10][16] as well as biosensor applications [17] could benefit from coatings preventing cell and bacterial adhesion.

2 Wetting and superhydrophobicity

The primary parameter characterizing wetting is the static contact angle, which is the measurable angle between a liquid and a solid. Factors affecting the contact angle include surface roughness and the chemistry of the surface, as well as the manner of surface preparation and the cleanliness of the surface. Value of the static contact angle for a hydrophilic surface is between 0 and 90 degrees, whereas for hydrophobic surface it is between 90 and 180 degrees. The terms hydrophobic and hydrophilic were originally applied only to water (‘hydro’ means ‘water’ in Greek), but it now is often used to describe the contact of a solid surface with any liquid. Oleophobicity/-philicity is sometimes used when referring to the wetting of a surface with an organic, non-polar oil. Surfaces with high energy, formed by polar molecules have the tendency to be hydrophilic, whereas those with low energy and built of non-polar molecules tend to be hydrophobic. If a surface displays a contact angle higher than 150 degrees it is defined as a superhydrophobic surface. [8]

2.1 Contact angle hysteresis

Another parameter characterizing surface hydrophobicity is the contact angle hysteresis which is defined as the difference between the advancing and receding contact angles. In sessile drop measurements, adding liquid to the drop causes the drop contact line to advance, and each time motion ceases the drop exhibits an advancing contact angle. Alternatively, if liquid is removed from the drop the contact line and angle decrease and the receding value of the contact angle is obtained. For a droplet moving along a solid surface (a tilted surface for example) advancing and receding contact angles are defined as the contact angle at the front of the droplet (advancing contact angle) and the back of the droplet (receding contact angle). It has been argued that the two definitions are not equivalent but in many cases they have the same meaning. [8]

The presence of hysteresis becomes critical with regards to superhydrophobic surfaces, since the self cleaning effect also requires low contact angle hysteresis. High hysteresis can also disguise superhydrophobicity, as it causes water drops to stick to the surface, though the static contact angle might be over 150º. Surfaces with low contact angle hysteresis also have a very low water roll-off angle, meaning the angle to which a surface must be tilted in order to roll off drops of water and “clean” the surface. The geometry of the surface features, such as the surface area in contact with the composite interface and the sharpness of the edges of the features, affects the hysteresis as well as the static contact angle. There

have also been attempts to prepare sticky superhydrophobic surfaces mimicking the adhesion behavior of gecko feet [18]. [19]

2.2 Wetting of smooth surfaces and Young's equation

Wetting describes the spreading of liquids on a solid surface resulting from intermolecular interactions. Controlling the wettability of solid materials is a classical key issue in surface engineering. Two situations are often of interest: complete wetting in which a liquid brought into contact with a solid spontaneously forms a film (superhydrophilicity), and complete drying, in which a liquid drop remains spherical developing no contact with the surface preventing liquid contamination of the solid surface. The degree of wetting depends on the surface tensions of the interfaces (surface-liquid, surface-air and air-liquid) involved and it is described with the contact angle, which is the angle between the liquid-air interface and the solid-liquid interface (Figure 2). [8] Young's equation [21] is the basis of all wetting phenomena and a drop fulfilling it is said to be partially wetting the substrate.

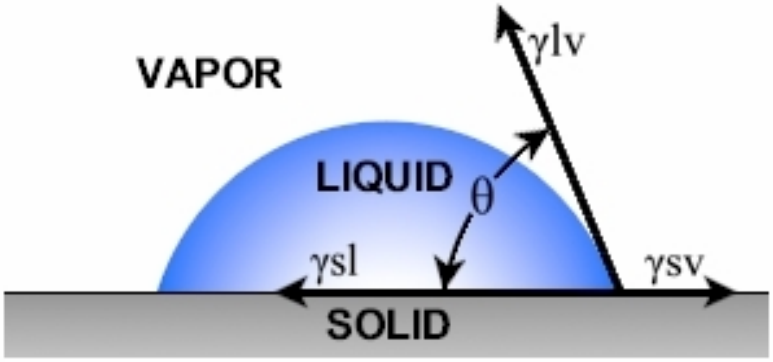

Figure 2 Definition of the contact angle on a flat surface [20]

Surface tension, denoted as γ_{IJ} for an interface between phases I and J, is the specific energy carried by surfaces which reflects the cohesion of the underlying condensed phase (either a solid or a liquid surface). It is defined as energy per unit area and thus force per unit length which applies along the surface to minimize the corresponding (positive) surface energy. Basic laws describing it were established for ideal solids which are both flat and chemically homogenous. A drop of water placed onto a solid will spread providing that the surface tension in the solid/air interface γ_{SA} is larger than the sum of solid/liquid and liquid/air surface tensions $\gamma_{SL} + \gamma$. This is because both of these surface tensions resist the spreading of the water expanding the two corresponding surface areas. [8]

Projecting on the solid plane the different surface tensions acting on the contact line provides the equilibrium condition of the drop, also known as the as Young's equation [21].

$$\gamma_{SA} = \gamma_{SL} + \gamma \cos\theta \quad (1)$$

Largest achievable contact angle on fluorinated materials, which are the most hydrophobic solids, is approximately 120◦ [22]. Contact angle values between 120◦ and 180◦ can be achieved by including roughness to the solid surface. [8]

2.3 Effect of surface roughness on hydrophobicity

Most solid surfaces, even the seemingly flat ones, are often rough at micrometric scale. Roughness may be generated during the fabrication process, such as coating or compaction of grains. Very few solids are molecularly flat, usually resulting from solidifying a liquid film, either free or suspended on another liquid. Defects, both chemical heterogeneities and roughness, on a solid surface can pin a contact line resulting in contact angle asymmetry as front and rear of the drop contact non-wetting and wetting defects. This asymmetry creates a Laplace pressure difference between the drop edges and thus, a force able to resist gravity making droplets on an incline stay at rest provided that the drop is small enough. [8]

The process of liquid deposition affects the contact angle since drop gently deposited on a surface spreads and stops when it is surrounded by primarily non-wetting defects and evaporates after a while, thus making its configuration that of a drop pinned on wetting defects. Contact angle hysteresis on rough surfaces can be exploited for example to guide a flow along a predefined route determined by a line of defects but it can also be unwanted as in the case of window panes in which drops of water stuck on them distort their transparency and contribute to the degradation of the glass. As crucial understanding the factors affecting contact angle hysteresis is, it is not yet clear which microscopic laws govern it causing the phenomenon in the macroscopic scale. [8]

2.4 Superhydrophobicity

Two key characteristics of superhydrophobic surfaces in terms of achieving the self-cleaning effect are a large contact angle (over 150°) of the fluid drop on the surface and the ability of the drop to roll off or move easily (low contact angle hysteresis, by definition

less than 10°). There are typically two states in which a drop can reside on a given rough surface depending on whether it sits on top of the surface roughness on air pockets or wets the grooves as seen in Figure 3 (b and c). The situation in which the drop is wetting the grooves is known as the Wenzel state and the apparent contact angle is given by Wenzel's formula. In the case of air pockets forming under the liquid on a rough surface, the surface is said be in Cassie state. [8]

Theoretical analysis has shown that, of the two possible states, a drop placed on a surface will behave according to the one it has the lowest energy in the system. The state of a drop on a surface is thus determined by geometric parameters of the surface roughness [23][24]. In both of these wetting theories for rough surfaces, the apparent contact angle is determined by two parameters, one of which is geometric (roughness ratio r) and the other one related to material properties (equilibrium contact angle θ). Depending on how the drop is formed, it can be in either Cassie or Wenzel state on the same rough surface, e.g. a drop in Cassie state can be forced to wet the grooves by applying pressure to it. From experiments it is known that drops in Cassie state show less contact angle hysteresis, in other words roll off the surface more easily, than the ones in Wenzel state which is due to the wetting of the grooves [25].

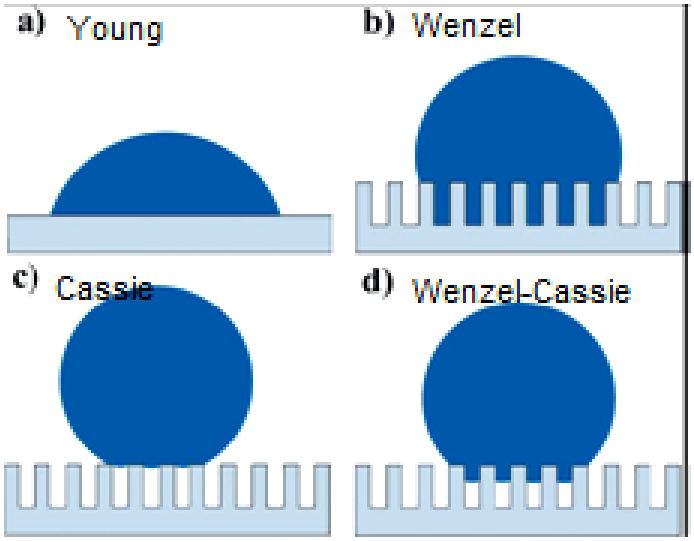

Figure 3 Effect of surface structure on the wetting behavior of solid substrates a) A drop of liquid on a flat substrate (Young's mode). b) Wetted contact between the liquid and the rough substrate (Wenzel's mode). c) Non-wetted contact between the liquid and the rough substrate (Cassie's mode). d) Intermediate state between the Wenzel and the Cassie modes [3].

In Wenzel [27] theory, the apparent contact angle is very sensitive to the material parameter, in contrast to the Cassie-Baxter theory [4], according to which the apparent

contact angle is fairly insensitive to material contact angle. Consequently, Cassie theory allows more control over the apparent contact angle, independent to the material contact angle, meaning that more different materials can be used to achieve desired apparent contact angles. It also renders the surface less sensitive to changes in material contact angle due to imperfections and contamination. [26]

2.4.1 Wenzel model for describing the effect of surface roughness

Surface roughness impacts the contact angle hysteresis, but also the apparent contact angle which was first discovered by Wenzel [27] using a geometrical argument based on the roughness factor, *r*, a ratio between the actual surface area and the apparent surface area of a rough surface. Wenzel model is based on the assumption that a fluid in contact with a rough surface completely wets the surface. As a result, the actual area between the liquid and the solid is greater than the apparent contact area (the area on the plane of the macroscopic surface). Wenzel's equation:

$$\cos\theta_W = r\frac{\gamma_{SL} - \gamma_{SV}}{\gamma_{LV}} = r\cos\theta \qquad (2)$$

According to equation 2 roughness enhances wettability, so if the factor *r* is larger than 1, a hydrophilic solid ($\theta < 90^\circ$) becomes more hydrophilic when surface roughness exists ($\theta_W < \theta$). Conversely, the hydrophobicity of a rough hydrophobic solid ($\theta > 90^\circ$) is increased. Contact line pinning is particularly strong in this state, both on the edges of and along the defects, as the liquid conforms to the roughness, which makes it difficult to check directly whether the relation is being followed. Also, if a Wenzel drop is moved along the surface, it will leave behind cavities filled with liquid which can also pin the drop. As a consequence, a drop in Wenzel state generally has very low receding angle and consequently very high contact angle hysteresis (rendering the surface "sticky") and thus, it is very difficult to detect the sole angle θ_W or to check if equation 2 holds true. [8]

2.4.2 Cassie model for describing the effect of surface roughness

Cassie and Baxter [4] used a similar approach to study the effect heterogeneous surfaces have on apparent contact angle. If the solid is hydrophobic and rough enough, the situation will be different from the Wenzel model. According to the model, liquid placed on the surface cannot be expected to conform to the solid surface, but rather air pockets should form below it. This state is called the Cassie state and it assumes that the energetic cost

associated with all the corresponding liquid/vapor interfaces is smaller than the energy gained from not following the solid. Cassie equation:

$$\cos\theta_C = f\cos\theta + f - 1 \quad (3)$$

Superhydrophobicity can be achieved by chemical surface modification together with controlling the density as well as height and diameter of the surface structures. The required density of the surface structures can be represented by the micro three phase contact line density from which the necessary surface forces to suspend the liquid against the forces of gravity can be obtained. Surface features must be tall enough to prevent the liquid from reaching the underlying solid and the diameter of individual feature has to be small enough to reduce the solid/liquid contact area. [3]

2.4.3 Superhydrophobicity in underwater conditions

Superhydrophobicity in air is characterized by a high apparent contact angle of a water droplet and contact angle hysteresis, but these criteria cannot be applied to underwater superhydrophobicity, since they are meaningless for a plate dipped into a liquid [28]. Samples remain immersed in culture media throughout the cell culture experiments so discussing the theory of underwater superhydrophobicity is relevant. Instead of contact angle, the only direct criterion that can be applied for underwater superhydrophobicity is the area fraction of the solid that is wet at equilibrium, $ø_e$, and thus the goal for underwater superhydrophobicity is to design a surface with $ø_e$ as small as possible, meaning in practice that the liquid touches only the tops of the roughness asperities, without penetrating into the roughness grooves.

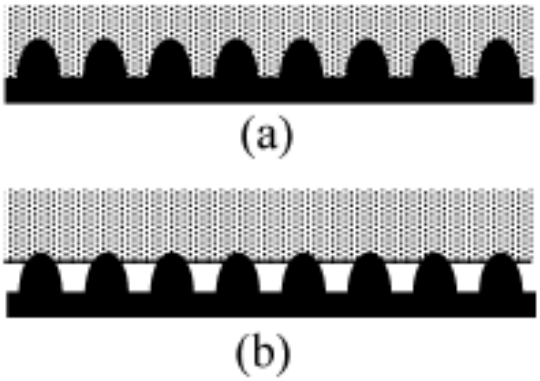

Figure 4 Wetting regimes of a rough surface: (a) homogeneous wetting, (b) heterogeneous wetting [28]

The predictions of surface roughening for the relevant range of Young's contact angle θ_Y (the largest achievable value is 120°, however 110° is a more realistic value) are presented in Figure 5, showing that stable underwater superhydrophobicity is possible with a sufficiently high roughness ratio (preferably about 3 for θ_Y = 110°). In practice, such roughness ratios are very difficult to achieve with random roughening processes, but structured surfaces (eg. Surfaces constructed of pillars) may produce such roughness values. The case of equilibrium partially inside the roughness grooves cannot be studied in general, since the results depend on the specific details, but the main issues can be demonstrated using a simple case, such as a surface composed of adjacent two dimensional semicircular protrusions.

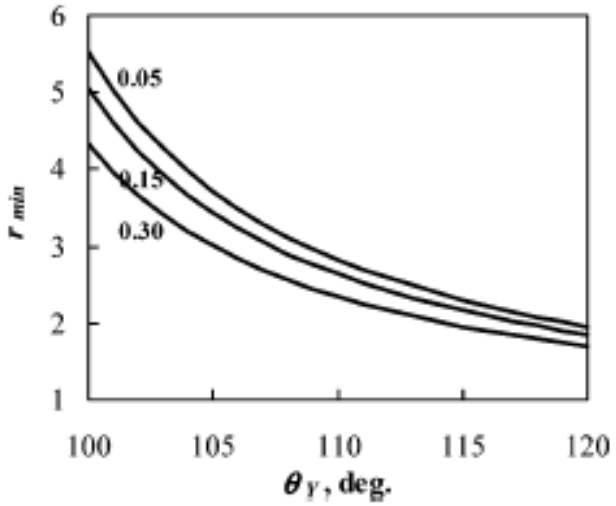

Figure 5 Minimum required roughness ratio in order to ensure a stable equilibrium state, for which the liquid-air surface is at the tops of the roughness asperities. [28]

3 Fabrication of superhydrophobic surfaces

Top-down approaches refer to fabricating materials and devices by carving, molding, or machining bulk materials with tools and lasers [29]. In order to create superhydrophobic surfaces template [30] and lithographic approaches [1][31], micromachining [32] and plasma treatments have been used. In contrast to the top-down methods, bottom-up approaches involve the building (or designing) larger, more complex objects by integration of smaller building blocks or components. In nanofabrication these techniques often involve self-assembly and self-organization, meaning that components spontaneously assemble in solution or the gas phase until a stable structure of minimum energy is reached. Bottom-up methods applied to the fabrication of superhydrophobic surfaces include chemical deposition methods such as chemical bath deposition (CBD) [33],

chemical vapor deposition (CVD) [34] and electrochemical deposition [35] layer-by-layer (LBL) deposition via electrostatic assembly [36], colloidal assembly [37] sol–gel methods [38] hydrogen bonding [39] and chemical synthesis [40].

The advantages of the bottom-up approach include the molecular control of the chemistry, composition, even the thickness of the product, but it is still difficult to predict the hydrophobic properties until the last step [12]. Superhydrophobic surfaces based on random surface roughness (e.g. Sol-gel surface) are more relevant from a practical perspective, because they are cheaper to fabricate. Similar to the designed rough surfaces, they also contain surface features on various length scales enhancing the superhydrophobic effect and making the surfaces less vulnerable to damage [29].

3.1 Sol-gel technology

Sol-gel methods enable powerless processing of glasses, ceramics and thin films or fibers, directly from solution at ambient temperatures. Mixture of liquid reagents (sols) leads to formation of gels which after drying produce glasslike, typically transparent and porous materials called xerogels (xeros – dry). The process can be described as the creation of an oxide network by progressive condensation reactions of molecular precursors in a liquid medium [41]. Precursors for the material are mixed at the molecular level and variously shaped materials may be formed at much lower temperatures than it is possible by traditional preparation methods. Sol-gels have a long history as the first papers on them were published over 150 years ago, however over the last decades the rapid development of this technology has opened a broad range of possible applications of sol-gel derived materials and biomaterials which marks this technology as one of the most promising fields of contemporary material sciences [42**]**.

3.1.1 Sol-gel materials

Sol-gel processes allow making ceramic and glass materials doped with of various inorganic, organic and biomolecules during the formation of a glassy matrix. Classical silica glasses as well as multicomponent materials combining silicates with titanates, borates and variety of other oxides (Zn, La, Al, Li, B, K, etc.) can be produced using sol-gel technology based on various alkoxides. Also certain nonsilicate oxide materials, such as ZrO_2, can be produced using the alkoxide gel method. [41]

Sol-gel derived materials have a broad range of possible applications as biomaterials which can be seen from the increasing number of publications in the literature. For biomedical

applications, benefits of sol-gel technology include low processing temperature combined with the intrinsic biocompatibility and environmental friendliness. In addition, with sol-gel technology it is possible to manipulate the structure of materials at the molecular level as well as precisely control the nature of interfaces which makes it an interesting approach for a wide range of practical applications. The sol–gel-derived materials provide excellent matrices for entrapping a variety of organic and inorganic compounds [43] and they have been demonstrated to have potential as substrates for adherent mammalian cells [44][45][46].

3.1.2 Chemistry of the sol-gel process

Sol-gel process involves the transition of a system from a liquid 'sol' into a solid 'gel' phase. Generally, the sol–gel process has four stages: (1) hydrolysis, (2) condensation and polymerization of monomers to form chains and particles, (3) growth of the particles, (4) agglomeration of the polymer structures followed by the formation of networks extending throughout the liquid medium which results in thickening and gel formation. There are two ways to prepare sol–gel materials: the inorganic method and the organic method. Usually the starting materials for the preparation of the sol are inorganic metal salts or metal organic compounds, such as metal alkoxides [M(OR)*n*], where M represents a network forming element such as Si, Ti, Zr, Al, B, etc, and R is typically an alkyl group.[41] Alkoxides are compounds formed by combination of a metal M with an alkoxide group OR, where R designates an alkyl group and they are characterized by the existence of M-O polar covalent bonds in their molecules [47].

Hydrolysis reaction
≡ Si-OR + H2O → ≡ Si-OH + ROH

Alcohol condensation
≡ Si-OH + RO-Si → Si-O-Si ≡ + ROH

Water condensation
≡ Si-OH + HO-Si → Si-O-Si ≡ + H2O

Figure 6 Hydrolysis and condensation in the process of preparing sol-gel silica derived materials [48]

The most commonly used precursors in sol–gel processes are tetramethyl-orthosilicate (TMOS) and tetraethyl-orthosilicate (TEOS). The solid gel is formed as the result of a polymerization process involving the establishment of M-OH-M or M-O-M bridges

between the metallic atoms M of the precursor molecules. Sol-gel transformations are equivalent to the polymerization process well-known to occur in organic chemistry consisting of the establishment of direct bonds between the carbon atoms of organic precursors. [47]

Silica based sol-gels are popular materials. Their production process includes several steps starting from mixing the silicate precursor (e.g. TEOS or TMOS) with water and a mutual a solvent (mostly alcohol) in the presence of acid or base catalyst and stirring the solution for a few hours. During this phase hydrolysis of the Si–O–R bonds occurs which can be catalyzed by acids (HCl, HF etc.) or bases (NH_4OH, NaOH etc.). After the hydrolysis has been initiated, generally also the condensation reactions occur simultaneously with it. [42]

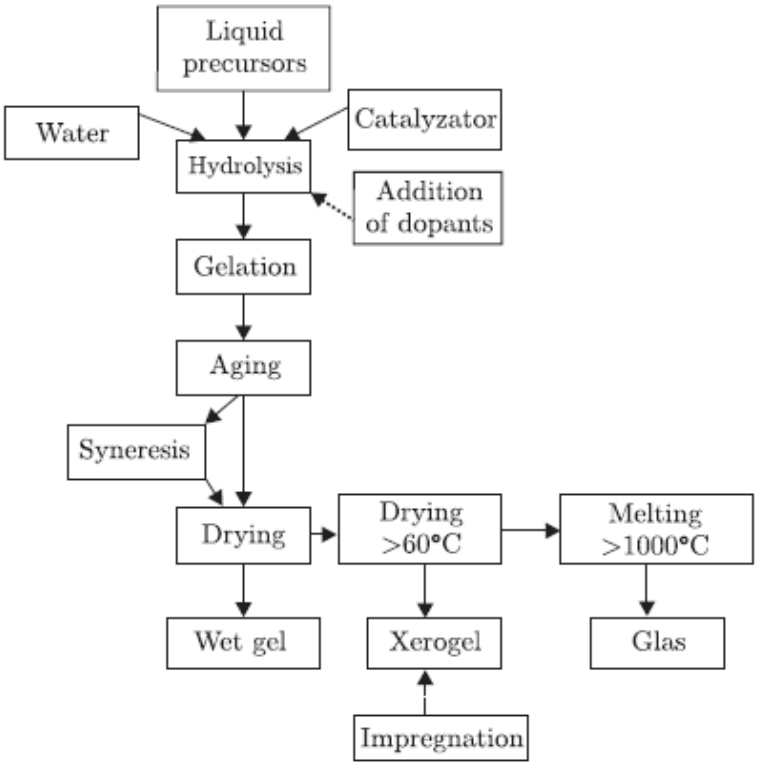

Figure 7 Conventional sol-gel process [42]

During the hydrolysis silanol groups (≡Si–OH) are formed and condensation reactions produce siloxane bonds (≡Si–O–Si≡) which results in the production of alcohol and water as by-products (Figure 6). The properties and composition of the final material depend strongly on the chemical reactions taking place during process [42]. The choice of the acidic or basic catalyst governs the promotion of hydrolysis or condensation reactions of

alkoxy silane, and thus influences the microstructure and the macrostructure and consequently the properties sol-gel materials [41]. Between the gelation and aging steps liquid is extracted from the gel in a process called syneresis [42]. The whole sol-gel schematically presented in Figure 7.

3.1.3 Gel structure

If the drying process is carried out at ambient pressure and at a temperature below 100 °C the solvent liquid is removed with substantial shrinkage and the resulting material is known as a xerogel, which are relatively sturdy, typically transparent but porous materials. The pore size of xerogels depends on such factors as time and temperature of the hydrolysis and the kind of catalyst used. During the drying process the gel volume decreases even several times and pore diameter is directly related to the shrinkage of the wet gel. When solvent is removed under hypercritical (supercritical) conditions the gel network does not shrink and a highly porous, low-density material called aerogel is produced [47]. Silica aerogels are extremely light, brittle materials, but still sufficiently strong to be handled. Their compressive strength, tensile strength, and elastic modulus depending they largely on the network connectedness and aerogel density, are very low [47]. Aerogel networks are often described as fractal geometrical architecture. [49] Xero- and aerogel structures are presented in Figure 8.

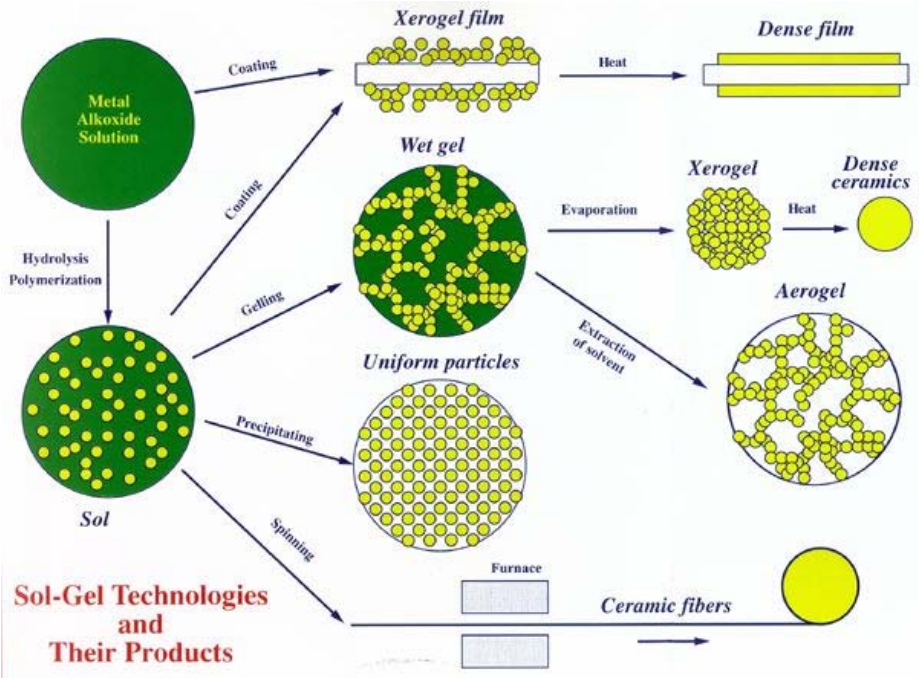

Figure 8 Structure of xerogels and aerogels [50]

3.1.4 Preparation of aerogels without supercritical conditions

Superhydrophobic aerogel films have been previously prepared by supercritical solvent extraction [51], which is a process requiring high pressure and temperature. Using these conditions can be circumvented by using ionic liquids as a solvent, but these liquids have been reported to be exotoxic [52]. Eutectic liquids composed of mixture of salts have similar properties to ionic liquids (capability to lower melting point and thus process temperature) and such liquid composed of choline chloride and urea in 2:1 molar ratio can be used to form silica aerogel films with optical transparency and superhydrophobic characteristics. Compared to ionic liquids used, eutectic liquids are cheaper to make, much less toxic and environmentally friendly (sometimes even biodegradable) and permit liquid mixture properties to be tuned by choosing different materials. [53] In the sol-gel process eutectic liquid serves as low vapor pressure, low melting point liquid and a templating agent. Superhydrophobicity and transparency are achieved by careful control of film thickness, surface roughness and a fluoroalkylsilane surface treatment of the ready-made silica film [54].

3.1.5 Coating methods

Sol-gel materials can be made in different configurations by further processing of the sol. Thin films can be prepared by dipping, spinning or spray coating and applied for large or irregular surfaces. Sol-gel transformation gradually increases the viscosity of the solution as the sol becomes interconnected to form a rigid, porous network of gel which can also be converted into dense ceramic or glass particles with further drying and heat treatment. [48]

Spin coating is a process of depositing thin film by centrifugal draining and evaporation which can be divided into four stages: deposition, spin-up, spin-off and evaporation [55], although in the case of sol-gel coatings, evaporation normally overlaps the other stages. Excess liquid deposited on the surface flows radially outward during the spin-up stage, driven by centrifugal force and as the process enters the spin-off stage the liquid flows to the perimeter of the substrate and leaves it as droplets. Film uniformity is due to the balance between the centrifugal force and the viscous force or friction driving the liquid flow inward. As the film becomes thinner its resistance to flow increases which slows down the removal rate of excess liquid by spin-off. In the final stage, thinning of the film is further continued by evaporation as the primary mechanism. [56] The advantage of spin-coating is that the film of liquid usually becomes uniform during the spin-off and tends to

remain that way, providing the viscosity of the liquid is not shear dependent and does not vary over the substrate [57].

In dip coating the substrate is dipped vertically into the coating bath and drawn back from it at a constant speed. As the substrate is moving, it entrains the liquid in a viscous boundary layer that splits in two at the free surface and returns the outer layer to the bath. As the substrate moves, the solvent is evaporating and draining and within the thinning film, inorganic species are concentrated, leading to aggregation, gelation and final drying. [58]

3.2 Organic-inorganic hybrid materials

Sol-gel technology also makes it possible to synthesize hybrid organic-inorganic materials which facilitate the design of new engineering materials with exciting properties for a wide range of applications. These materials are called ORMOSILS (ORganically MOdified SILicates), ORMOCERS (ORganically MOdified CERAMics) and CERAMERS (CERamic polyMERs) or POLYCERAM (POLYmeric CERAMics) [42]. In sol–gel derived organic–inorganic hybrid materials, inorganic constituents are chemically incorporated into the organic network at the molecular level. This allows the advantages of inorganic materials, such as high mechanical strength, good chemical resistance, rigidity, high thermal stability, to be combined with the ones of organic polymers, including flexibility, lightweight, good impact resistance high dielectric constant, ductility and processability. [59]

3.2.1 Fabrication of hybrid materials

Methods for preparing hybrid materials can be classified into three major approaches according to the chemical bond between inorganic and organic phases: (1) The organic component can be directly mixed into the inorganic sol–gel system, making the end product is a simple mixture with no chemical bonding between organic and inorganic components; (2) Already existing functional groups within the polymeric/oligomeric species can be made to react with the hydrolyzed of inorganic precursors, thus introducing chemical bonding between them; (3) alkoxysilanes R’n Si(OR)4−*n* can be used as the sole or one of the precursors of the sol–gel process with R’ being a second-stage polymerizable organic group often carried out by either a photochemical or thermal curing following the sol–gel reaction. [60]

3.2.2 Process parameters affecting structure and mechanical properties of hybrid materials

Hybrid materials produced in a sol-gel process can be tailored to have a wide range of physical attributes, depending on the type and amount of substrate used and other variables such the process conditions like pH and temperature. The degree of phase dispersion and consequently on many chemical parameters such as organic-inorganic ratio, molecular weight of macromonomers, number of anchoring groups, reactivity of cross-linking alkoxide reagents and processing, solvent, define the properties of the hybrid networks and even slight changes in these parameters can cause wide variety in the material. [60]

3.2.3 Crosslinking

Generally, mechanical properties of hybrid materials are determined by the nature and the nanoscale size of the filler (silica), the hybrid interface and the nature of the interactions between the organic and inorganic components. Increasing the TEOS content of these materials increases the elastic modulus and stiffness of these materials since it increases the number of crosslinking points, which enable the hybrid network to become more and more crosslinked and thus stiffer.[61] For example incorporating organoalkoxysiloxanes in the silicate matrix reduces the degree of cross-linking, improves film adhesion to its supports and the mechanical properties of sol–gel matrix. Polydimethylsiloxane (PDMS) possesses desired properties such transparency, good chemical and thermal stability and similarity of its backbone structure (-Si-O-) to tetraethoxysilane and therefore PDMS/silica hybrid materials have been widely investigated having potential applications as non-linear optical materials, chemical sensors and protective coatings [59][62][63][64].

3.3 Fluoroalkylsilane coatings for achieving low surface energy

Fluoroalkylsilane (FAS) molecules possess a dual nature which causes one end of the molecule to react with a surface and the other end to have non-wetting functionality. The fluoroalkylsilane molecule is bifunctional as its silane termination will bond to many different types of substrates while the other end has a highly fluorinated chain terminated with a CF_3 group (Figure 9) which has the tendency to orient itself away from the surface, forming a tightly packed, low-energy release surface [65]. These surfaces have many interesting tribological properties as non-stick coatings and they have been suggested for adhesion control in biomedical application. [66]

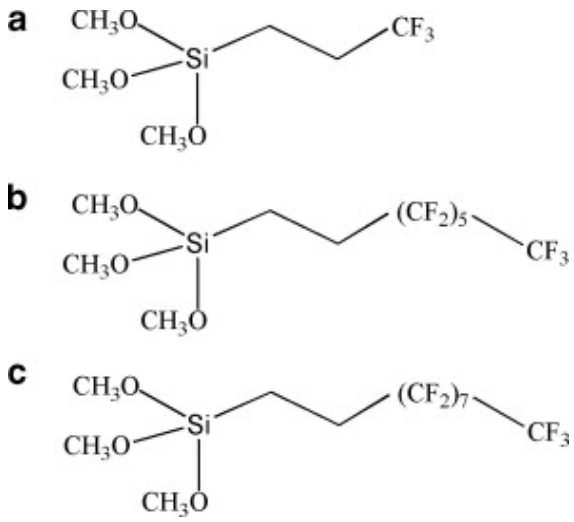

Figure 9 Chemical structure of some fluoroalkylsilane molecules (a) (3,3,3-trifluoropropyl)trimethoxysilane, (b) 1H,1H,2H,2H-perfluorooctyltrimethoxysilane and (c) (Heptadecafluoro-1,1,2,2-tetrahydrodecyl)trimethoxysilane [66]

3.3.1 Properties of fluoroalkylsilane coatings

Fluoroalkylsilane coatings are very stable because F-C bonds are one of the most stable ones and the bulky fluorine atoms also cover the carbon atoms beneath the surface, preventing the chemical attack on weaker C-C bonds. Fluoroalkylsilanes have also been reported to form self-assembled monolayers (SAMs) which contain a well ordered structure with a controllable organic functional group on the surface [67] (Figure 10). Fluoroalkylsilane monolayers are also attractive because their preparation is very simple and the film thickness can be precisely controlled by changing the length of the fluoroalkyl chain. [66]

Fluoroalkylsilane coatings alone are both highly hydrophobic and oleophobic, which is unique when compared with other coatings. They have been found effective in preventing water penetration [68] and corrosion [69] and they have also shown to have superb wear resistance and friction reduction properties [70]. Fluoroalkylsilane coatings have demonstrated good biocompatibility, most likely due to their extremely low surface energies (approximately 8 mJ/m^2) [71] and coated surfaces are capable of preventing the adhesion of most chemical and biological substances [72]. Coatings have been proven to be effective in reducing the adhesion and growth of bacteria [16][73][74][75], as well as

the growth of astrocytes and choroid plexus cells (cell types found in the central nervous system) [10].

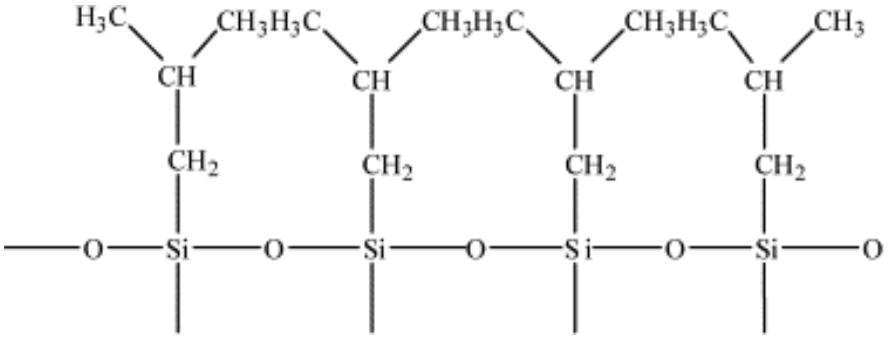

Figure 10 Illustration of hydrophobic groups on a fluoroalkylsilane treated surface [76]

3.3.2 Cell and bacterial adhesion to fluoroalkylsilane coatings

Wang et al. [77] evaluated the short- and long term inflammatory reaction caused by silicon and sapphire wafers with and without FAS SAM coating in the brain. Implants were placed on the surface of adult rat cortex for 10, 28, and 90 days. The brain tissues directly under the implanted wafers were analyzed histologically and specific evaluations of the cell types that contribute to an inflammatory response were used. Smooth fluoroalkylsilane coating was found to remain stable and to successfully reduce inflammatory response caused by sapphire implanted in the central nervous system of rats for up to 90 days. However, applied on silicon surface, the same coating failed in vivo after 10 days, which was attributed to the corrosion of the underlying silicon substrate.

Stenger et al. [78] were able to direct the polarity of embryonic hippocampal neurons by manipulating the patterns of aminosilane self-assembled monolayers (SAM) on a background of FAS. Neurons avoided the areas coated with FAS which suggest that FAS reduces cell growth. Based on these results, Patel et al. [10] coated silicone disks with FAS coatings in order to see whether this coating would reduce cell adhesion and thereby prevent cell migration into the cerebrospinal shunt lumen, and thus prevent shunt obstruction and failure. FAS-coated surfaces exhibited less astrocyte proliferation compared to polystyrene, heparin- and hyaluronan-coated surfaces and they also showed lower cell growth compared to unmodified silicone. Similar results were obtained with choroid plexus epithelial cells strengthening the hypothesis that hydrophobic surface coating may reduce cell adhesion.

Wang et al. [16] evaluated the adhesion of Staphylococcus epidermidis on fluoroalkylsilane coated silicone for 4, 8 and 12 hours and showed reduced adhesion compared to untreated silicone. Based on these observations, the superhydrophobic fluoroalkylsilane coating studied in this thesis, might be even more effective in reducing cell and bacterial adhesion.

3.3.3 Stability of fluoroalkylsilane coatings in physiological conditions

Patel et al. [10] also conducted contact angle measurements on FAS coated silicone before and after immersion in saline solution (0.9% NaCl) at 37°C for 0, 5, 10, 20, and 30 days, which showed that the coating remained hydrophobic. These results, together with degradation studies by Wang et al. [16][77] (Figure 11) suggest that fluoroalkylsilane coatings remain stable in physiological conditions and are thus suitable for long term in vivo use.

	Elemental Composition (%)									
	C		O		Si		N		F	
Sample	Control	5 days	Control	5 days	Control	5 days	Control	5 days	Control	5 days
Silicone	47.6		26.9		25.5					
OTS/silicone	50.4	48.3	24.8	29.7	24.8	22				
Heparin/OTS/silicone	50.8	50	25.2	24.6	20.4	21.9	3.6	3.5		
Hyaluronan/OTS/silicone	49.2	49.5	26.3	26.3	20.9	20.7	3.6	3.5		
FAS/silicone	24.3	25.7	21.5	20.2	13	12.7			41.2	41.5

Figure 11 XPS analysis of fluoroalkylsilane (FAS, lowest on the table) coating on silicone before and after immersion in saline [16]

4 Cell and protein adhesion to biomaterials and its implications for implant performance

Biomaterials used for manufacturing *in vivo* implants and medical devices must satisfy certain performance criteria including biocompatibility and long-term stability. Biocompatibility can be defined as the ability of the material, intentionally placed within the body for transient diagnostic or therapeutic purposes to be able to perform its intended function without inducing uncontrolled activation of cellular or plasma protein cascades [79]. The surface structure of the implant should not cause the denaturation of adsorbed proteins and proinflammatory reactions of microvascular endothelial cells [80].

Cell adhesion and integration to surrounding tissues is desired for many implants, such as orthopedic implants and tissue engineering constructs, but for example in the case of catheters, stents and biosensors, cell adhesion can prevent the implant from working properly. Also macrophage adhesion activates the immune system and resulting in foreign body reaction which can have devastating consequences to the material surface (Figure 12) can be devastating and device function [9]. Surface modification or coating with anti-adhesion properties are thus needed.

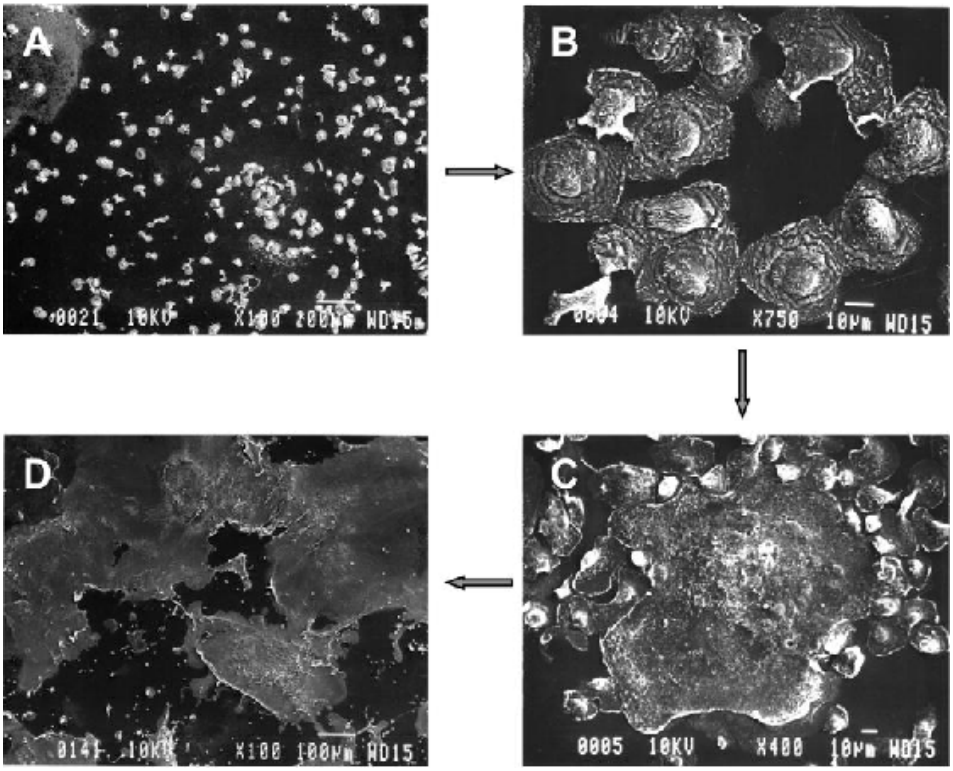

Figure 12 Scanning electron microscopy images of an implanted Elasthane 80A Polyurethane surface showing monocyte adhesion after 0 days (A), monocyte-to-macrophage development after 3 days (B), ongoing macrophage-macrophage fusion after 7 days (C), and foreign body giant cells after 14 days (D), showing also the damage to the material. [9]

4.1 Biocompatibility

Biocompatibility is mediated by cell–cell, cell–surface and surface–protein interactions and it is essentially a surface phenomenon. The degree of biocompatibility of a material is a sum of a number of parameters, the most important including: the type of material, the genetic inheritance of the patient; the site of implantation and the contact duration. The factors that depend on the material include the following: shape, size, surface chemistry

and roughness, design, morphology and porosity, composition, sterility issues and nature of degradation. The intensity and duration of the tissue reaction is based on these parameters and in order to develop suitable materials for biomedical applications, the structure and chemistry of the solid–liquid interface of the material and the biological environment it is placed should be thoroughly understood. [81]

4.2 Biomaterial-tissue interaction

Mechanisms of implant acceptance and/or integration are complex and still poorly understood, but tissue responses to materials can be divided into four major categories [82]. All of these interactions stabilize the implant but may lead to different complications and problems.

(1) The material releases some toxic compounds leading to necrosis to the surrounding tissue.
(2) The material is non-toxic but is gradually being resorbed and replaced by the surrounding tissue.
(3) The material is non-toxic and biologically inactive, but cannot be degraded by the host and so it reacts by encapsulation.
(4) The material is non-toxic but increasingly interactive with the surrounding tissues in forming chemical bonds with it.

4.3 Protein adsorption as a mediator of cell attachment

Protein adsorption is a fundamental aspect of biocompatibility since it is well known that cell interaction with materials implanted into the human body is mediated by a layer of proteins from blood and interstitial fluids layer, which influences subsequent cell adhesion and activation. This layer covers the surface immediately after implantation, and thus it is the adsorbed proteins, rather than the surface itself, to which cells initially respond. Proteins in an unrecognizable state may indicate that a foreign material is to be removed or isolated. In order to manipulate cell adhesion, the physical surface properties can either be altered to modulate the ability of the surface to capture proteins from solution, or alternatively, proteins can be directly deposited onto a surface. Because of the complexity of the interface and difficulties in its characterization, understanding of cell–biomaterial interactions is a work in progress, but it is still possible to identify a number of key elements in the system and their likely modes of action. [83][84]

Surfaces hindering or completely blocking early protein adsorption process would also reduce cell growth and prevent pathogens from attaching onto the surface. Antifouling surfaces would be beneficial for surfaces that cannot be cleaned for extended periods, such as some biomedical devices. [85] Protein adsorption is usually rapid on flat hydrophobic surfaces and bound proteins are most likely altered by the interaction with the surface. [86] Highly hydrophilic surfaces have been shown to reduce protein adsorption but it has also been suggested that superhydrophobic surfaces could prevent it due to the to the reduction of surface are in the solid-liquid interface (according to Cassie model)

4.3.1 Protein adsorption mechanisms

Proteins are extremely surface active presenting high affinity for interfaces [87][88][89] and the typical surface-associated concentration has been estimated to be in the order of 1000 times that in solution. [90] Protein adsorption may be promoted or opposed by a number of potential enthalpic and entropic changes within the surface–water–protein system. These changes can be divided into three groups [91]:

1. (Partial) dehydration of protein and sorbent surfaces
2. Redistribution of charged groups in the interface
3. Conformational changes in the protein molecule

The nature of the protein, sorbent, and solvent determine, which of these three processes is dominant.

4.3.2 Dynamics of protein adsorption

Adsorption will increase in time at least until the coating approaches monolayer coverage, after which it begins to decrease in relation to the number of available binding sites [][92] becoming progressively more dependent on the protein–surface affinity. However mixed solutions such as blood might have different adsorption behavior.[83] Competitive protein adsorption is a key determinant of cell response to surfaces and which proteins adsorb from serum or plasma to a limited number of binding sites will depend on their relative concentrations and surface affinities. [93][][94]

Cell adhesive serum proteins, such as fibronectin and vitronectin, play a critical role in cell adhesion to an artificial material [107][84]. Albumin is the most abundant serum protein (concentration 100–1000 times higher than those of fibronectin and vitronectin) and it is expected to preferentially adsorb onto the surfaces during the early phase of the formation

of an adsorbed protein layer but it is also later expected to be displaced by cell adhesive proteins such as fibronectin. [95]

4.3.3 Vroman effect

If there are no cells present, the composition of the adsorbed layer will generally change over time as faster diffusing molecules (e.g. albumin) are displaced by proteins with a higher affinity for the surface, a phenomenon often referred to as the Vroman effect. [90][96][97][98] The Vroman effect states that the ratio of proteins adsorbed on the surface of a biomaterial in the first few seconds is proportional to their ratio in the adjacent protein solution, but as equilibrium is reached in minutes to hours, the ratio becomes proportional to the proteins relative affinity to the surface. The effect is most pronounced on hydrophilic surfaces onto which proteins are typically less tightly bound [] and it is often associated with serial displacement rather than simple desorption [][99].

4.4 Cell adhesion onto biomaterials

Cells change their shapes and expand metabolic energy in order to stabilize the interface between their membrane and the underlying materials by both physicochemical and biological mechanisms [100]. Cell adhesion to material surface defined as a two-step mechanistic process: the first stage is controlled by complex combinations of physico-chemical interactions including hydrophobic, coulombic and van der Waals forces between the cell membrane and the material surface [101]. The first stage can be characterized as "passive adhesion" according to this adsorption mechanism compared to the second stage which might be considered as active adhesion, since it involves of the participation of cellular metabolic processes. An ideal surface would be one with continuity in chemical and physical structure and properties. Cell culture systems are used to evaluate material biocompatibility before introducing them to in vivo testing and clinical use. [100]

Adhesion to extracellular matrix is essential for the survival of most cell types, including connective tissue cells such as fibroblasts and initial cell attachment to a material surface determines the subsequent processes such as cell adhesion, spreading, morphology, migration, proliferation and differentiation [83]. The growth of a cell and its phenotypic behavior are partly regulated by its ability to adopt an appropriate morphology, thus making the nature of cell adhesion to any substratum a critical determinant of a whole suite of cell, and ultimately tissue, responses [102][103][104][105][106]. Cells in their natural environment are anchored to their surroundings by discrete attachments to proteins in the

extracellular matrix. Similar to this, cells in vitro attach to culture surfaces via adhesion proteins contained in serum-supplemented culture medium [107][108].

4.4.1 Integrins

Cells and adhesion proteins interact primarily via integrins, which are heterodimeric receptors in the cell membrane. They are approximately 10 nm wide and the most abundant receptor type on the cell membrane, being 10–100 times more prevalent compared to other types [109]. Most cell interactions with extracellular surfaces are mediated by integrins since they control all major cellular activities, including adhesion, changes in cell shape, proliferation and migration [110][111]. As cells adhere to ECM, integrins are clustered into focal adhesion complexes and intracellular signaling cascades into the nucleus and cytoskeleton are activated [112][113].

4.4.2 Mechanism of integrin binding

When integrins encounter an available binding domain in the ECM or artificial material, they undergo a conformational change leading to the recruitment of two groups of cytoplasmic proteins, one of which biomechanically connect them to the cytoskeleton and another that biochemically initiates or regulates intracellular signaling pathways. As multiple integrins physically cluster together, more cytoplasmic proteins are recruited to the adhesion site to increase its size, adhesion strength, and biochemical signaling activity. The resulting large structures of integrins and cytoplasmic proteins are called focal adhesions which are believed to regulate the cytoskeleton and act as centers of signal transduction. [114]

4.4.3 Focal adhesions

The formation, development, and disassembly of focal adhesions are key activities in cell spreading and migration and they also appear to be central modulators of many cellular functions such as cell proliferation and differentiation because of their ability to modulate intracellular signaling. Focal adhesions are scattered across the cell surface and are typically 0.25–0.50 μm wide and 2– 10 μm long, though they arise from much smaller clusters. Expression and distribution of integrins, and thus the nature of cell adhesion, may also be changed according to the ligands available [115][116][117] and the differentiation state of the cells. [118][119] Cells and their interfaces are dynamic systems which should be taken into consideration in addition to the initial states and it should be noted there is a

difference between the early adhesion process occurring when cells commence interaction with the substrate, and the continuous adhering strength [120].

4.5 Effect of surface roughness and wettability on protein and cell adhesion

Surface properties of biomaterials, such as topography and wettability, are critical factors for protein and cell adhesion. Many cells adhere to extracellular matrices in vivo, having a complex 3D topography in the micrometer-to-nanometer range [121]. Surface morphology interferes with the assembly of the focal adhesion points, which affects not only cell adhesion but also differentiation, proliferation, matrix production, cell morphology, and orientation [122]. Cells respond to microscale features by altering their shape, such as elongating along grooves. [123][124] In contrast, appropriately scaled nanoscale features have been shown to prohibit cells from forming focal contacts and thus prevent cell adhesion. [125][126] Wettability changes resulting from surface roughness, in other words topography, are likely to contribute to these cellular responses.[127]

Since the surface curvature of nanoscale surface roughness is close to protein molecular dimensions, it reduces the contact area unless the protein molecules deform. [128] Studies on the effects of surface morphology on cell adhesion have given contradictory results, as some have shown that nano- and microtopography and, in particular roughness, increase cell adhesion [129][130][131] while others revealed the opposite behavior [132][133]. Topography has thus been concluded to be able to influence cell adhesion and spreading both positively and negatively, depending not only on the properties of the surface but also on the cell type, as showed by a recent study by Khor et al. [134].

4.5.1 Micro - and nanoscale surface features

The effects of microtopography on cell adhesion, contact guidance, and cytoskeleton organization has been studied extensively [135] and more recently also nanoscale dimensions have shown increasing importance in controlling the cell response to biomaterials [84]. Wojciak-Stothard et al. [136] discovered that P288D1 macrophage-like cells react down to dimensions at least as small as 44 nm and epithelia, fibroblasts, and endothelia cells have been demonstrated to respond to depths as shallow as 70 nm [135]. Cell response to micron-sized features is closely connected to the behavior of the cytoskeleton, but the existence and nature of a receptor on the surface of the cell membrane linking the sequence of effects has not yet been established [124], though stress receptors have been suggest to be responsible [137].

Fibroblasts and Mesenchymal Progenitor cells (MPCs) have been shown to react to surface features as small as 10 nm [138] and it seems that both of these cell types adhere and therefore proliferate better on nanofeatures that are wormlike than dot-like [134]. Nanopatterns with height less than 10 nm appeared to elicit different rates of adhesion and proliferation in fibroblasts and mesenchymal precursor cells. Calvalcanti-Adam et al [139] reported that the size of one integrin in the cell membrane is between 8 and 12 nm and they also investigated the relationship between the distances between gold nanoparticles each binding one integrin and cellular adhesion. Closely spaced nanopatterns (58 nm) showed the best cell adhesion in the case of rat fibroblasts [139].

4.5.2 Selective cell adhesion caused by nanoscale surface features

Nanoscale topographic features seem to also affect the selectivity of cell adhesion since the adhesion of fibroblasts in comparison to that of osteoblasts seems to be reduced in nanostructured surfaces whereas on microstructured surfaces these two cell types demonstrate the same affinity ratio [140]. Similar results have been reported with other cell types such as smooth muscle cells and chondrocytes. Biomaterials selectivity to cell adhesion could have important implications in specification of tissue responses at bone and mucosal surfaces of for example dental implants. Nanophase materials have also been shown to have decreased bacterial adhesion and proliferation. Reduced bacterial colonization has been demonstrated on nanostructured $Ti0_2$ and Zn0 though they simultaneously promote osteoblast adhesion and differentiation which could be further explored in terms of biofilm accumulation and peri-implantitis in dental implants.

4.5.3 Effect of surface wettability to protein adsorption

Surface wettability is one of the most important factors influencing protein adsorption. Water is a polar solvent which does not readily interact with nonpolar solutes and surfaces, and hence contact between water and these hydrophobic surfaces increases self-association (by hydrogen bonding) within the neighboring water molecules.[141] Acidic, basic, polar, and nonpolar amino acid side chains of a protein interacting with water and each other create the folded structure of a protein, with hydrophobic residues preferentially located toward a water-excluding core of the molecule [][142], but in spite of this protection of hydrophobic residues, Haynes and Norde [] estimated that 40–50% of the accessible surface of small proteins is occupied by nonpolar groups. In order to a protein to adsorb onto a surface both adsorbate and surface must at least partially dehydrate [][143][144], which by increasing water's entropy is a thermodynamically favorable for similarly hydrophobic sorbents and adsorbates [][][145].

On hydrophilic surfaces, it appears that the displacement of water molecules presents a substantial energy barrier to protein adsorption. [][] Surfaces with tightly bound water have shown significantly less or none protein adsorption [146] but on the other hand there is also evidence that adsorption does occur on hydrophilic materials, where charge interactions and protein conformation changes provide the necessary driving force. It is presumed that since a greater number of adsorption-promoting interactions are possible, hydrophobic surfaces usually adsorb more proteins than the hydrophilic ones [147][148][149], though it cannot be considered an universal result as some proteins have been reported to display a high charge dependent surface affinity.[150] In some studies, hydrophilic and hydrophobic surfaces have been shown to adsorb similar amounts of protein in the absence of competition [151]. In the case serum proteins of hydrophobic surface displaying contact angles above 100° albumin is barely displaced by cell adhesive proteins because of its stronger adsorption on the surfaces, whereas it is easily replaced by cell adhesive proteins on relatively hydrophilic surfaces. [95]

4.5.4 Effect of surface wettability on cell adhesion

Several surface properties influence cell response to biomaterials including surface charge, topography, hydrophobicity or hydrophilicity, surface chemistry and surface energy. Today it is generally accepted that the polar and dispersion components of surface free energy have an impact on the adhesion and spreading of cells. [152] A number of studies have focused on examining how cell behavior and bioadhesion is influenced by surface energy, in other words hydrophobicity or hydrophilicity. Cells have been observed to adhere, spread (flatten) and grow more on the surface areas with moderate hydrophilicity, with a maximum adhesion of cells at a water contact angle of approximately 57◦, with all studied cell types (Chinese hamster ovary, fibroblast and endothelial cells) and also the serum proteins adhered better onto these areas of moderate hydrophilicity. Wettability seems to play a dominant role especially in the initial period of cell-material interaction, but with prolonged exposure time the chemical composition of a surface might be more crucial for cell proliferation [46]

4.5.5 Optimal wettability for enhanced cell adhesion

Tamada et al. [153] claimed that a polymer surface with a water contact angle of 70° is most suitable for cell adhesion, however, the surfaces used in these studies were prepared using commercially available polymers and were not well controlled for factors of roughness, ionic charges, surface rigidity, etc. Lee et al. [154] examined cell adhesion to

polyethylene surfaces with a gradient of wettability prepared by the corona discharge and found the maximum cell adhesion was achieved at a water contact angle of 55°. Ruady et al. [155] used chemically defined gradient surfaces of dichlorodimethylsilane (DDS) coupled to glass and found that cells preferentially adhered in the region on the gradient with advancing water contact angles around 50°.

In most studies done on the effect of surface wettability, not only the wettability but also by the functional groups on surface, surface density, roughness, and rigidity are varied. Therefore, it is difficult to discriminate between the effects of surface wettability and those due to other surface properties on cell behavior. To gain deeper insight into the true effect of surface wettability Arima et al. [95] used mixed self-assembled monolayers (SAMs) of alkanethiols with different terminal groups to evaluate the effects of wettability on the adhesion of human umbilical vein endothelial cells (HUVECs) and HeLa cells (epithelial cells) which adhered well on moderately wettable surfaces with water contact angles of 40–60° as reported in the previous studies using various polymers and the number of adhering cells decreased as contact angle was increased from this. It was demonstrated that cell adhesion to materials is mainly determined by surface wettability, but is also affected by the surface functional groups and its density, as well as cell type in question.

4.5.6 Predicting cell adhesion with wettability models

The wetting responses of surfaces with different topographies can be described with the Wenzel and Cassie-Baxter equations, but ideally it would also be desirable to predict the effect of topography on bioadhesion. Carma et al. [] examined the how cellular responses are linked to wettability models basing their hypothesis upon the assumption that wettability influences the contact sensing of living cells which is a part of the fouling processes. Cell culture experiments with endothelial cells on geometrically patterned poly(dimethyl)siloxane demonstrated, that if cells are too large to rest between or on top of the features, they must bridge, align, or conform to their shape. This suggests that cell responses are governed by the same underlying thermodynamic principles as wettability.

Bridging is similar to the air pocket state and alignment is similar to the wicking states described by the Cassie-Baxter relation, in contrast to conforming to surface morphology which resembles Wenzel behavior. If a surface, for which an organism has a relatively low affinity, is topographically engineered to expand the Cassie-Baxter regime, then the organism may be induced to bridge over the features. Bridging increases the tension along the unsupported regions of the organism's membrane and is also expected to reduce the area of contact between the organism and surface reducing the overall adhesion strength.

Thus, bridging of the cells over surface features creates unfavorable energy barriers and reduces potential for cell settlement. Though wettability models are important in predicting cellular adhesion onto engineered topographies, they do not fully explain the process. Adhesion is a complex and species specific process since the material modulus and surface elasticity of the cell membrane are other factors to consider, in addition to the variety of adhesive proteins, glycoproteins, and polysaccharides that organisms secrete. [127]

4.6 Protein and cell adhesion onto superhydrophobic surfaces

Although extensive work has been done showing that cellular responses to surfaces are markedly influenced by water wetting behavior of substratum materials, only a small number of papers has explored the superhydrophobic range. Most of these studies, show reduced or no cell adhesion, but Senesi et al. [156] actually reported increased cell adhesion. The literature on protein adsorption in general is controversial and inconsistent, and the situation is the same for superhydrophobic surfaces for which some studies report protein-adsorbent properties and others non-adsorbent properties. To get a better understanding of the phenomena in biological setting, this chapter summarizes the studies published so far on protein and cell adhesion on superhydrophobic surfaces.

4.6.1 Protein adsorption onto superhydrophobic surfaces

Zhang et al. [157] showed that while proteins dissolved in water did adhere to superhydrophobic surfaces, the adsorption was often slower than on flat surfaces. This reduced adsorption rate may be due to protein conformational changes required before attachment or the hydrophilicity of the adsorbed layer driving the solvent front into the surface structure, allowing water and protein to penetrate. [158] They also showed that almost complete removal of protein films occurred from some of their superhydrophobic surfaces (nanostructured sol-gel silica with fluorocarbon coating) under flow conditions. Larger scale superhydrophobic surfaces were shown to have the opposite effect, causing increased adsorption, which might explain the mixed results achieved by other studies. Superhydrophobic surfaces might not be able to prevent protein adsorption entirely, but reduce the binding strength and therefore allow easy the removal of bound proteins by flow shear or other methods. [85]

When superhydrophobic surfaces are immersed in water, air bubbles are entrapped into micro- and nanosized surface features. This air bubble layer creates a barrier that may prevent adsorption of cells and bacteria in the short-term. As immersion time increases,

organisms displace the air on the surface, so the key for designing superhydrophobic surface for long term prevention of biofouling is to make the surface effectively 'hold' the air in place. Air trapping capability of a surface depends on the roughness and the design of the air adsorption sites. Loss of superhydrophobicity during long term submersion can occur because the air dissolves into the water or be due to changes in the chemistry or structure of surface, caused by the attachment of a conditioning layer of macromolecules. [157]

4.6.2 Fibroblast adhesion and spreading on superhydrophobic FEB-teflon

The first cell culture study conducted on a superhydrophobic material was by Schakenraad et al. [159] who studied the adhesion and spreading of human fibroblasts on hydrophobized and hydrophilized FEP-Teflon, and compared it with adhesion and spreading on untreated FEP-Teflon and tissue culture polystyrene. Superhydrophobic FEP-Teflon was prepared by ion etching followed by oxygen glow-discharge whereas the hydrophilic FEP-Teflon was prepared by ion etching only. Modified surfaces displayed contact angles of 140-150-degrees (hydrophobic variant) and 5-10-degrees (hydrophilic variant) whereas for untreated FEP-Teflon contact angle was 109-degrees. Human skin fibroblasts displayed a significant decrease in spreading on the superhydrophobic FEP-Teflon as compared to untreated FEP-Teflon whereas cell spreading on hydrophilic surface was increased. Since oxygen glow discharge was used in the production of the superhydrophobic surfaces, the surface chemistry of the analyzed hydrophobic and hydrophilic surfaces should therefore have some differences.

4.6.3 Culturing cells on superhydrophobic surfaces

Superhydrophobic surfaces might have a potential use in the field of cell culture, since mammalian cells do not seem adhere on them. Ino et al. [2] applied a superhydrophobic film to culturing cells and as cells did not adhere to it, the film was used developed two novel culture methods: a droplet cell culture as an easier method of producing embryonic stem cell or mesenchymal stem cell aggregates using a superhydrophobic surface and also allocated cells on micropatterned surfaces consisting of superhydrophobic regions and cell culture-treated regions. Superhydrophobic surfaces were fabricated by using microwave-plasma-enhanced chemical vapor deposition (MPECVD) to form thin films with nanotextured surfaces of approximately 300 nm thickness and vacuum ultraviolet (VUV) lithography was applied to fabricate the superhydrophobic/hydrophilic pattern in which the hydrophilic regions were of glow treated tissue culture polystyrene.

Cell patterning methods are important for constructing in vivo like-tissue organs such as vascular structures so in addition to droplet cell culture, in this study several kinds of cells were allocated using a micropatterned surface consisting of superhydrophobic regions and cell-culture-treated regions. Culturing human umbilical vein endothelial cells (HUVECs) and mouse 3T3 cells on the surface patterned with hydrophilic (contact angle approximately 66°) and superhydrophobic (contact angle over 150°) regions showed that the HUVECs did not exhibit the normal spread morphology on the superhydrophobic surface areas, whereas the cells adhered and extended on the cell-culture-treated ones. 3T3 cells proliferated within the hydrophilic region, but did not extend into the superhydrophobic region (Figure 13).

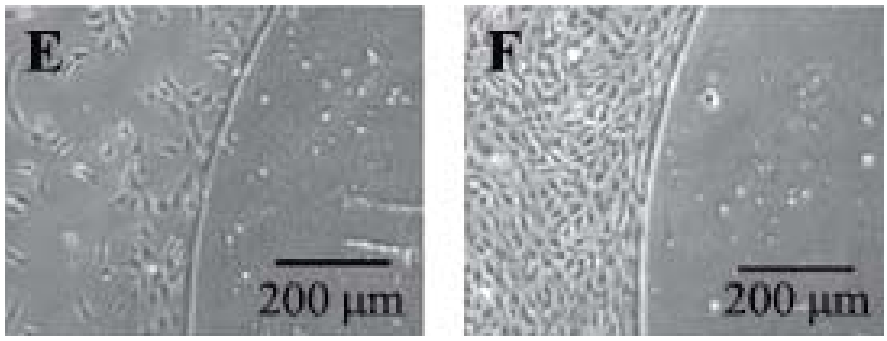

Figure 13 3T3 cells were seeded onto the hydrophobic/hydrophilic pattern on the superhydrophobic surface, and cultured for 1 d (E) and 3 d (F).

4.6.4 Cell adhesion to superhydrophobic poly(L-lactic acid)

Alves et al. [14] produced poly(L-lactic acid) (PLLA) surfaces with superhydrophobic characteristics (contact angles 154° ± 4°) based on the Lotus effect, exhibiting dual micro- and nanoscale roughness. Cells have previously been show to be able to adhere, proliferate, and differentiate on PLLA [160]. The second passage of rat bone marrow derived cells was used to evaluate the cytocompatibility of the PLLA surfaces. For the superhydrophobic surface the number of cells was considerably lower after 3 days of culture compared to the smooth control surface with the same surface chemistry (Figure 14).

Also, the shape of the cells adhering to the surface was different, as the cells exhibited a much more round shape and were attached to the solid substrate through cytoplasmatic projections in just a few points. The authors hypothesized this could be a result of the fact that the medium suspension was not effectively in contact with the entire surface, as predicted by the Cassie and Baxter model. They also conducted a longer direct contact test and for the superhydrophobic substrate virtually no cells could be found. A single cell

detected in one sample exhibited a spherical shape. These findings strengthen the hypothesis that, even if some cells can hold onto the superhydrophobic surface in the initial period, the superhydrophobic character of the surface compromises cell adhesion and proliferation. [14]

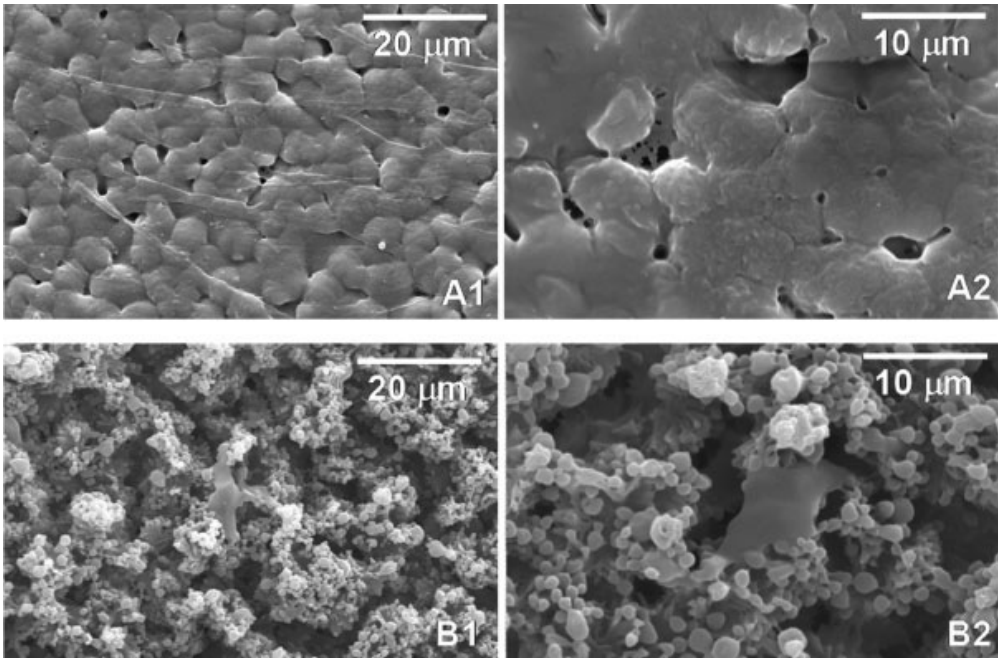

Figure 14 RBMCs onto (A) smooth films (A1 and A2 with different magnifications) and (B) superhydrophobic substrates (B1 and B2 with different magnifications, showing a single cell in the middle of the image), after 3 days of culture [14].

4.6.5 Stem cell response to superhydrophobic TiO_2 nanotubes

Bayer et al. [161] studied the cell response of mesenchymal stem cells to strongly hydrophobic and super-hydrophobic surfaces obtained via organic modification of TiO_2 nanotubes with self-assembled monolayers of octadecylphosphonic acid (ODPA). They grew self-organized layers of vertically orientated TiO_2 nanotubes providing defined diameters ranging from 15 up to 100 nm on titanium foils by anodic oxidation and consequently modified their surface with a self-assembled monolayer of ODPA. Modified nanotubes showed a diameter-dependent wetting behavior ranging from hydrophobic (108° ± 2°) up to super-hydrophobic (167° ± 2°), in other words the degree of wettability was altered while all other physiochemical properties at the surface remained constant. Cell adhesion was considerably enhanced after 24 h on super-hydrophobic surfaces, but this effect disappeared after 3 days. The authors did not distinguish whether the decrease in cell number is due to inhibition of cell proliferation or cell apoptosis. Based on the

adsorption experiments with ECM proteins, this temporary effect could not be explained with the specific adsorption of those proteins on methyl-terminated self-assembled monolayers.

4.6.6 Cell attachment to superhydrophobic polydimethylsiloxane

Khorasani et al. [100] studied the attachment of anchorage dependent cells, namely baby hamster kidney (BHK) fibroblastic cells, on CO_2-pulsed laser modified polydimethylsiloxane (PDMS) with different hydrophobicities. Virgin PDMS exhibits hydrophobic behavior and relatively poor wettability with the contact angle of 105°. CO_2-pulsed laser treatment changed the surface wettability by increasing the contact angle with increasing pulse number up to 5 pulses resulting in superhydrophobic surface (θ = 175 ±5◦) above which the contact angle decreased. This was attributed to the high hydrophobicity and porosity of the surfaces after the laser treatment.

BHK Cells have fibroblast-like morphology and they only grow in mono-layer culture. After 24 hour incubation, their adhesion and spreading was lower on treated PDMS with rough porous surface than on the untreated, smooth and non-porous control. Cells on the rough PDMS also became smaller and had round morphology. Cell edges did not appear attached and filopodia growth was minimal compared to BHK cells on the smooth untreated PDMS which were flattened and displayed small peripheral filopodia and ruffled edges. In addition to making the surface rough and porous, laser treatment changes the chemical composition of the surface by producing hydroxyl, carboxyl, and carbonate groups. These are oxygen rich groups with negative charge which probably also contributes to the reduced cell adhesion. Based on the observed small and round cell morphology, it appears that only passive adhesion (only hydrophobic, coulombic and van der Waals forces between the cell membranes and the surfaces) takes place in the attachment of BHK cell to the treated PDMS surfaces. [100]

4.6.7 Increased cell growth, adhesion and spreading on a superhydrophobic polyethylenetherephtalate with fluorinated surface structures

Though all of the other summarized studies reported reduced or no cell adhesion on superhydrophobic surfaces, Senesi et al. [156] showed that superhydrophobicity actually increased cell adhesion, spreading and growth. These surfaces were nanostructured ‘‘teflon-like’’ coatings with highly-fluorinated, random, ribbon-shaped, micrometers-long structures, deposited on polyethylenetherephtalate (PET) substrates by plasma enhanced-chemical vapour deposition (PE-CVD). 3T3 fibroblasts cells were cultured on flat (115° ±

5°), hydrophobic (130° ± 5°) and super-hydrophobic (160° ± 5°) nano-structured samples and the sample surface area covered by cells was evaluated by optical microscopy analysis at different times (3 h, 24 h, 48 h, and 96 h). A higher number of cells and a better cell morphology (adhesion, spreading and growth) were obtained at the greatest nano-structure heights, surface roughness and water contact angle values. The authors did not provide any explanation on the increased adhesion, though it was contradictory to other cell culture studies done on other superhydrophobic surfaces.

4.7 Blood compatibility of superhydrophobic materials

Blood clotting is part of human body's natural defense mechanisms. Any surface coming into contact with blood is considered an intruder by blood components and thus, initiates the clotting process, of which goal is to isolate the foreign object. Blood clotting is a complex process composed of a cascade of chemical pathways initiated by the activation of several proteins, Factor XII, plasma prekallikrein, Factor XI and high-molecular-mass kininogen (HMM-kininogen). This leads to a chain reaction which results in the activation of platelets that bind to the surface and recruit more platelets to form a blood clot. Since blood coagulation is a surface reaction, which can only take place at the interface of the foreign material and blood, it has been hypothesized that reducing this contact area would lead to reduced clotting and better biocompatibility. This would be a very valuable property to biomedical devices exposed to blood, both inside and outside the human body. [26]

4.7.1 Strategies for improving blood compatibility

Blood contacting medical devices experience problems due to platelet adhesion and activation on material surfaces leading to blood coagulation and thrombosis which may be life-threatening or cause functional failure. Numerous approaches have been developed to fabricate more blood-compatible materials, such as nonthrombogenic endothelial cell and chemical modifications, but since these methods strongly rely on chemical synthesis or biological treatments, their use is often confined to specific materials. Interactions between the coagulation system and biomaterial surfaces are of a highly complex nature as they involve plasmatic enzymes as well as cellular elements and flow conditions. [162]

Usually heparin in administrated to prevent coagulation on the biomaterial surface when using them in direct contact with blood for a short time (e.g., for blood circulation, catheterization, drainage, and temporary blood passage during surgical operation).

However, using such an anticoagulant is not recommended especially when the patient is prone to hemorrhage by drug administration at high concentration and thus it is important to develop a better understanding on how to manipulate platelet–surface interactions to increase the thromboresistance of the foreign surface toward blood [163]. Since platelet adhesion to a biomaterial surface results in the formation of a hemostatic plug or thrombus, platelet adhesion and platelet number counting is one of the most popular experimental tools for evaluating the hemocompatible properties of synthetic materials [26]. Several strategies have been proposed to avoid blood coagulation and thrombus formation through surface modification and thus improve the blood compatibility of biomaterials which include creating highly hydrophilic and hydrophobic blood-material interfaces [164][165][166].

4.7.2 Hemocompatibility of superhydrophobic carbon nanotube coating

Sun et al. [167] reported a novel nanostructural effect on blood compatibility, which provides a convenient but general strategy to improve the hemocompatibility of various ordinary biomaterials through simply introducing special nanostructures making them superhydrophobic. Two kinds of Poly(carbonate urethane)s (PCUs) with different ratios of fluorinated alkyl side chains were coated with aligned carbon nanotube (ACNT) films composed of densely packed multiwall carbon nanotubes, with an average diameter of about 39.7 nm and a length of about 20 mm, aligned vertically to the substrate. Platelet adhesion experiments carried out in vitro by using the platelet-rich plasma (PRP) method showed that almost no platelets adhered to the nanostructured materials, and immunofluorescence experiments further showed much less platelet activation compared with the corresponding smooth surfaces.

4.7.3 Effect of superhydrophobic modification of polytetrafluoroethylene (ePTFE) on hemocompatibility

Toes et al. [168] examined whether superhydrophobic modification improves the in vivo performance of small diameter expanded polytetrafluoroethylene (ePTFE) vascular grafts and patches which are frequently used to reconstruct occlusive diseased human arteries, particularly when no autologous material is available. Problem with the implanted grafts is the incidence of early and late occlusion is high, even when anticoagulation or anti-platelet therapy is used. Superhydrophobic modification did not lead to less neointima formation and resulted in significantly more platelet deposition than did standard ePTFE vascular grafts and thus it does not improve the performance of small diameter ePTFE vascular grafts. The results were contradictory to previous study by Schakenraad et al. [169] and the

reason for the discrepancy between remains thus unexplained. However, since superhydrophobic modification fails to improve the performance of small diameter ePTFE vascular grafts, they cannot be used in the human circulation

4.7.4 Effect of superhydrophobic modification of PDMS on hemocompatibility

Khorasani et al. [163] studied whether the modification of PDMS surface by laser irradiation and graft polymerization of hydroxyethylmethacrylate phosphatidylcholine (HEMAPC) reduced platelet adhesion onto it. They prepared surfaces with different wettability including untreated PDMS (hydrophobic), laser-treated PDMS (superhydrophobic, 170°), and HEMAPC-grafted surfaces (superhydrophilic) and evaluated platelet adhesion and activation onto these samples. Laser treatment created homogeneous porosity PDMS surface which has the typical dimension of about 400 nm. This is much smaller than the dimension of the platelets (3–5 um) and it should thus inhibit platelet trapping and further platelet activation.

PRP studies showed that platelet spreading was lower both on the laser-treated PDMS and on the HEMAPC-grafted PDMS compared to the unmodified surface which was completely covered by platelets and displayed microthrombi formations. Thus it could be concluded that these surfaces do not induce platelet activation. LDH activity measurements also showed that the CO2-pulsed laser-treated PDMS and HEMAPC-grafted PDMS surfaces have better results for blood compatibility compared to the unmodified one since two surfaces did not induce platelet activation and the numbers of platelets attached are less than the control sample. Better blood compatibility of the prepared superhydrophobic and superhydrophilic surfaces is due to both the roughness (porosity) and the charged chemical nature of the surface (oxygen enriched, negative charge) which serves to alter the properties to nonplatelet activity

5 Biofilm formation and infection

Biomaterial placed in the human body often becomes colonized with bacteria (i.e. biofilm forms), which eventually causes infection. The initial stage for the infection is the bacterial adhesion and protein (such as albumin, fibrinogen and fibronectin) adsorption onto the material surface. Proteins arrive to the surface within seconds from the implantation, which means that the following interaction of cells, including platelets, endothelial cells and fibroblasts, with the biomaterial is mediated by the adsorbed protein layer. Thus, the initial protein adsorption onto a biomaterial surface plays a key role in the host's response to the implant, making it crucial to understand the protein adsorption phenomena when designing

biomaterials. Bacterial adhesion is mediated by the surface physico-chemical properties of the implant material and after the initial adhesion the bacteria slowly proliferate and form a colony or biofilm which subsequently leads to systemic toxicity. [170]

Bacterial infections due to medical implants are common and potentially serious complications, typically leading to premature implant removal. Despite of preventive measures, such as sterilization, meticulous surgical procedure and proper infection control guidelines, invasive bacteria can be found at approximately 90% of implantation sites immediately after the surgery. Effective methods for preventing initial bacterial adhesion to implant surface and further biofilm formation would lead to less infections and better implant performance. [170]

5.1 Biofilm structure and processes

Biofilms have demonstrated to be highly hydrated open structures composed of 73–98% extracellular material and void spaces, such as pores and channels which are believed to serve as nutrient-carrying passageways maintaining bacterial viability and proliferation capacity in all the layers of the biofilm [171]. Biofilms also do not seem to be structurally homogeneous monolayers of microbial cells, but heterogeneous in both time and space formed of microcolonies serving the basic building blocks [172]. Understanding the physiological interactions of microcolonies within a developed biofilm is essential for interpreting basic biofilm processes, such as quorum sensing (sensing between bacteria to coordinate certain behaviors based on the local density of the population.), antimicrobial resistance and detachment [171].

Once attached, bacteria express genes in a pattern leading to phenotypic changes [173] and bacteria within the biofilm develop intrinsic resistance by gene activation, changing the cell envelope and molecular targets, and thus altering their susceptibility to antimicrobial agents [174]. This is why biofilms are structurally complex possessing a dynamic architecture and are thus able to develop on many abiotic surfaces [173]. Biofilm development consists of physicochemical and molecular interactions, proliferation of the primary colonizer and escape of adhering and non-adhering daughter cells [79].

5.2 Initial attachment to the surface

Bacterial attachment to material surface is due to physical forces, including Brownian movement, Van der Waals attraction, gravitational forces, surface electrostatic charges and hydrophobic interactions, as well as chemical factors [175]. Chemotaxis (direction of

movement according to a certain chemical) and haptotaxis (directional motility or outgrowth, usually up a gradient of cellular adhesion sites or substrate-bound chemoattractants) also contribute to the process of bacterial adhesion. Almost all microbes modulating their growth by regulating cellular adhesion components experience chemotaxis which prepares them for cell–cell and cell–surface interactions. Haptotaxis, also referred to as chemo attractant, originates from bacterial interaction with amino acids, sugars and oligopeptides [79].

Physical interactions bacteria experiences on a surface can be classified to long-range (more than 50 nm) and short-range (less than 5 nm) interactions. Long-range interactions cause the bacteria to be transported to the surface in the first place but at closer proximity the short-range interactions, arising from hydrogen bonds, as well as ionic and dipole interactions, become more predominant [176]. Long-range interactions are non-specific and a function of the distance and the surface free energy [79]. Biofilm evolution and the detachment of the cells can be regulated by population density-dependent gene expression, controlled by the cell-to-cell signaling molecules [177]. In addition to this, clumping factors, proteins and teichoic acid also contribute to the generation of highly viscous mass [175].

5.3 Bacteria proliferation and biofilm maturation

The second stage of biofilm formation involves the proliferation of the primary colonizers and the maturation of the biofilm. During this stage, the organism either multiplies without releasing progeny cells or primary colonizers recruit and co-aggregate bacteria of the same or different species. Simultaneously with this process, most bacteria produce extracellular polymeric substances (EPS), stabilizing the biofilm architecture. All organisms adopt different mechanisms for the formation and stabilization of the film [79]. Some may for example produce substances which reduce their own metabolic activity, making the bacteria less susceptible to the killing by antibiotics [178][179].

5.4 Spreading of the infection

After the initial adhesion, bacteria begin to generate slime which helps in colonization of the surface, protects against phagocytosis, interferes with the cellular immune response and reduces of effects of antibiotics [180]. 20kD acidic polysaccharide slime matrix acts as a physical and chemical barrier, protecting the sessile biofilm communities against antibiotics, in contrast to bacterial strains that do not produce slime and are rapidly killed

by the host immune system [79]. Chronic infections occur when the host's local defense system is overcome by the size of the bacterial inoculum [171].

Infection is spread via non-adhered cells and some of the adhered daughter cell, which escape from the slime layer either by switching off the slime production through a mechanism of phenotypic modulation, or by exhaustion conditions that support slime production, and are thus free to drift to new colonization sites to repeat the process of biofilm formation [174]. Nutrition starvation seems to a role in biofilm detachment as biofilms grown under continuous flow conditions causing nutrient starvation detach after flow is stopped [181].

5.5 Bacterial adhesion on superhydrophobic surfaces

Riekerink et al. [182] developed method to obtain superhydrophobic surfaces by means of treating low density poly(ethylene) (LDPE) films with radiofrequency (RF) tetrafluoromethane (CF4) gas plasma. Microbial adhesion experiments were performed in a parallel-plate flow chamber during a period of three hours using two different suspension buffers (phosphate buffer and phosphate buffered saline) and the fouling behavior of the films was screened by adhesion of several microbes (e.g. Staphylococcus epidermidis, Streptococcus oralis, Escherichia coli, Pseudomonas aeruginosa, Candida albicans). Microbial adhesion onto superhydrophobic fluorinated LDPE was compared to adhesion onto three reference materials (untreated LDPE, fluorinated ethylene propylene copolymer (FEP) and poly(ethylenimine) coated LDPE) and surprisingly, in most cases superhydrophobization of LDPE films did not lead to a substantial decrease of microbial adhesion. Modifying surface roughness and energy did not seem to affect the bioadhesive properties of the films, whereas inverting the film surface charge (from – to +) resulted in a much higher initial microbial adhesion.

6 Experimental part

Superhydrophobic coatings were prepared using the combination of a sol-gel method and fluoroalkylsilane treatment. This method was chosen because it provides an easy and affordable means to produce superhydrophobic coatings on multiple substrates of different shapes. Sol-gel coatings (non bioactive) have shown potential for cell culture and are non toxic. Smooth surfaces coated with fluoroalkylsilanes have been shown to reduce bacterial and cell adhesion and they have also proven to remain stable in physiological conditions for up to 90 days [183].

6.1 Materials and methods

First part of the materials and methods section focuses on the preparation and of the superhydrophobic coating as well as modifying the pure silica coating with PDMS in order to enhance its mechanical properties. In the second part, in order to demonstrate the potential of this coating for reducing or completely blocking cell and bacterial attachment, MG63 osteoblast like cells were cultured on the superhydrophobic surfaces, as well as smooth fluoroalkylsilane surfaces and silica aerogel thin films. MTT assay was also conducted to evaluate the toxicity of the different coatings.

6.1.1 Sample preparation

The superhydrophobic coating consists of two coatings, a porous SiO_2 film and a monolayer of fluoroalkylsilane. Solvent evaporation during the sol-gel process causes surface roughness of the resulting film, which combined with the low surface energy fluoroalkylsilane coating results in superhydrophobicity.

6.1.1.1 Silica coating

The general formulation for solution and film formation from the eutectic liquid is: tetraethoxysilane (TEOS $Si(OC_2H_5)_4$): 0.6 g, eutectic liquid:choline chloride-urea (mixed on a hotplate over night): 1.2-2.4 g, ethanol: 1.5-3 g, 1M HCI aqueous solution: 0.3g. Hydrolysis and condensation occurred after addition of HCl to the mixture, and stirring the solution vigorously for 15 minutes. Film uniformity was not very good on small glass slides, which were coated for cell culture experiments so a tri-block copolymer pluronic P123 (0.12-0.2g) was added to the sol to enhance wetting between it and the substrate during spin-coating process. This improved the ability of the film to uniformly cover the substrate.

Glass slides (VWR® Micro Cover Glasses, Round, No. 2, 18mm) disks were used as substrate material. Substrates were cleaned with ethanol and subsequently with UV-ozone for 10 minutes prior to spinning the sol on them (1000-1500 rpm for 15-30 sec) to form uniform films of thicknesses between 50 and 500 nm depending on the amount of ethanol. The coated glass slides were placed in a desiccator with a container of 1 ml ammonia (29%), to promote gelation. After 1 week, the slides were removed from the desiccator and rinsed extensively with ethanol to remove the eutectic liquid, and thus yield a porous thin film. The process is described in Figure 15.

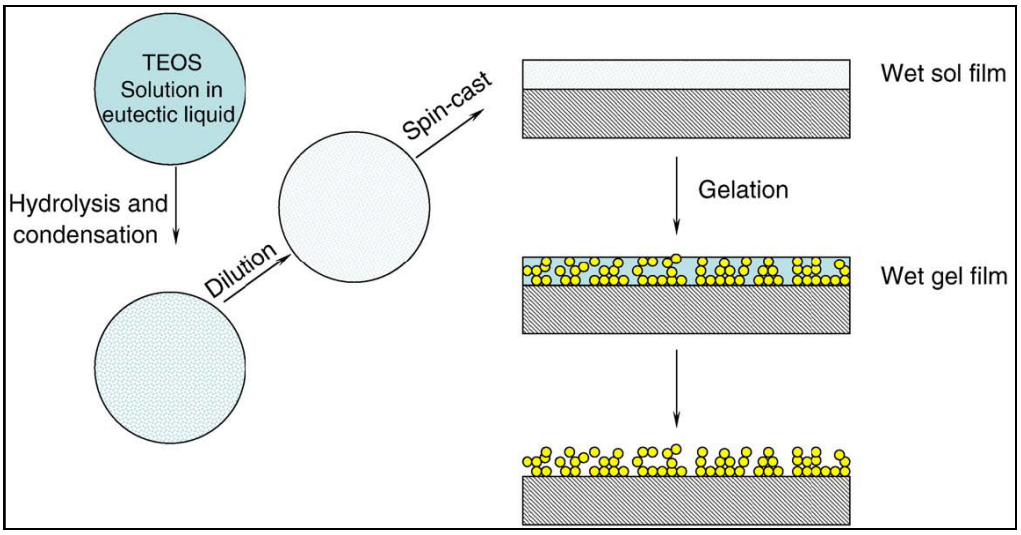

Figure 15 Schematic illustration of the procedure to prepare rough silica surface [184]

To investigate the applicability of the superhydrophobic coating on biomedically relevant materials, fine polished titanium alloy (titanium-6 wt% aluminum- 4 wt% vanadium alloy, Ti-6Al-4V) disks (15 mm in diameter) were also coated. Polishing to create the smooth surface was performed by lapping with 18T grit (oil based 500-600 grit aluminum oxide) followed by polishing with 4.0 paper (1200 grit aluminum oxide) by French Grinding Service, Inc. (Houston, TX). Disks were stamped using an automated metal punch and cleaned in an acetone bath using an ultrasonic cleaner for one hour. The disks were then washed in Jet-A fuel (grade AL-24487-F; Diamond Shamrock, San Antonio, TX) in an ultrasonic cleaner for one hour which was followed by four washes with Versa Clean (Fisher Scientific, Pittsburgh, PA). Between each wash with Versa Clean the disks were rinsed twice with deionized, distilled water. After the final wash, the disks were rinsed with 70% ethanol and then dried in vacuum. Prior to use each disk was washed again three times with ethanol and rinsed three times with deionized, distilled water. Prior to coating the disks were characterized with profilometry and XPS. Disks are referred to as Ti-A-S (A for the alloy and S for the smooth surface). [185]

6.1.1.2 Modifying the silica coating with Poly(dimethylsiloxane)

This silica-based superhydrophobic surface offers much potential in self-cleaning coatings for which optical transparency is required. However, the mechanical robustness must be improved for implementation in commercial products. One approach is to incorporate PDMS or some other polymer into the silica matrix.

Prepared silica coatings were glass-like and brittle, so TEOS-PDMS hybrid films containing different ratios (20, 30, 40 and 50 wt%) of PDMS were prepared in order to improve the mechanical properties of the films. Hydroxy terminated PDMS was added to the sol and the coatings prepared similarly to the silica films. TEOS/PDMS coatings were first prepared on the same glass slides see whether the surface roughness required for superhydrophobicity could also be created with this composition of the sol.

6.1.1.3 Dip coating

Since most of the possible biomedical applications (e.g. implants) for the superhydrophobic coating cannot be coated by spinning, dip coating was also used for preparing the sol-gel silica coating. No dip coating machine was available, so coating was done manually by dipping glass and Titanium surfaces into the sol. Samples were immersed in the sol (preparation described earlier) and kept there for 1 minute after which they were held up horizontally for 30 seconds to allow excess solution to drip off. After drying, dip coated samples were also treated with fluoroalkylsilane and water contact angles measured to verify superhydrophobicity.

6.1.1.4 Fluoroalkylsilane treatment

In order to achieve superhydrophobicity, the surface energy of the films was lowered by fluoroalkylsilane treatment. Ten millimolar solution of perfluorooctyl trichlorosilane (PFOS) was prepared in hexane ((trichloro(1H,1H,2H,2H-perfluorooctyl) silane, PFOS)/n-hexane) and the substrates with spin-cast silica films were placed in it for 30 min to allow adsorption of a PFOS layer onto the SiO_2 surface. Subsequently the samples were rinsed with isopropanol and heated to 150°C in air for 1 hour and 5 minutes in 220°C to promote silane hydrolysis and condensation, thereby forming a stable fluorosilanated layer on the silica surfaces.

6.1.2 Characterization of the coatings

Wettability of the coatings was determined with contact angle measurements. Scanning electron microscopy (SEM) and atomic force microscopy (AFM) were employed to examine the coating surface morphology and evaluate its distribution on the entire sample surface. The SEM technique may be considered as complementary to AFM since it allows evaluate the distribution on a small scale of homogeneity.

6.1.2.1 Contact angle measurements

Coatings were characterized by measurement of the water contact angle, an indicator of the wettability of surfaces, which was measured by a sessile drop method at room temperature using an optical bench-type contact angle goniometer (ramé-hart). Drops of purified water (4µl) were deposited on the surface on five different locations using a microsyringe attached to the goniometer and static images were recorded from which the contact angle of the droplet on the solid surface was determined.

The difference between the measured advancing angle and the receding angle is defined as the contact angle hysteresis which is related to the sliding angle so the hysteresis value can be used to characterize the self-cleaning effect of a superhydrophobic surface. Contact angle hysteresis was measured using 0.5 µl step changes on a microsyringe. Advancing contact angles were measured by increasing the volume of the 4 µl water droplet to 6 µl and receding contact angles subsequently by reducing the volume to 4 µl by extracting the extra water with a volumetrically controlled pipette using the same 0.5 µl step changes.

6.1.2.2 Scanning electron microscopy

For SEM inspection, the samples were fixed to aluminum stubs with conductive tape. Since the glass slides and the coatings were non-conductive, they were coated with a thin layer (~20nm) of gold using a plasma sputtering apparatus (Ernest Fullam) before SEM observation in order to prevent charge accumulation. Surface morphology was characterized with high resolution field-emission scanning electron microscopy (FESEM; LEO 1530 FEG and Hitachi 800) at 6–10 kV.

6.1.2.3 Atomic force microscopy and profilometry

Surface roughness was measured with AFM system (Veeco NanoScope IIIa/Dimension 3000) using the tapping mode. Profilometer (KLA- Tencor P-15) was used to assess the surface roughness of the Ti-A-S disks prior to coating them.

6.1.2.4 X-ray photo electron spectroscopy

In addition to micro/nano structured surface superhydrophobicity requires low surface energy, which is directly related to surface chemical composition. In order to verify the chemical composition of the surface, x-ray photo electron spectroscopy (Surface Science Instruments XPS SSX-100) was conducted.

6.1.3 Cell culture experiments

MG63 osteosarcoma cells were used to study the effect of the superhydrophobic coating and the two coatings it is composed of on the behavior of cultured cells. Cell numbers on different coatings on glass and Ti-A-S substrates were determined to evaluate attachment. Scanning electron microscopy was used to examine cell morphology on glass with different coatings.

6.1.3.1 MG63 human osteosarcoma cells

Osteoblast like MG63 cells were used because of their availability in the laboratory. MG63 cell line was originally derived from a male human osteosarcoma and represents a less differentiated stage of osteoblastic maturation. The line is a well established model for studying the effects of surface morphology on osteoblast-like cells. When cultured on tissue culture plastic, MG63 cells spread and have a fibroblastic morphology [185]. On smooth Titanium surfaces, they display a flattened morphology, while on rougher surfaces with R_a of 4-7μm, they show a more cuboidal morphology characterized by prominent cytoplasmic extensions.[186]

6.1.3.2 Experimental design for attachment test I

MG63 cells were used to evaluate cell adhesion to the superhydrophobic coating, which was hypothesized to prevent cell attachment.

Group 1: Tissue culture polystyrene (PCPS)
Group 2: Tissue culture glass
Group 3: Fluoroalkylsilane coated glass
Group 4: Silica coated glass
Group 5: Both silica and fluoroalkylsilane coatings (superhydrohobic)

The superhydrophobic samples in group 4 have two coatings, one to create surface roughness (thin film composed of silica particles, group 3) and another one to lower the surface energy (monolayer of fluoroalkylsilane, group 2).

Samples (six of each group) were put into 12-well plate and CellCrown inserts were placed on top of them to avoid possible floating. MG63 cells were plated into the wells at a density of 36,000/well in Dulbecco's modified Eagle medium containing 10% fetal bovine

serum (FBS) and 1% antibiotics (pen/strep). After 24h of incubation cell attachment and morphology was examined with optical microscope and cell number determined using optical and fluorescence microscopy.

After this, media was removed, cells washed twice with PBS ((1x PBS; 13 mM NaCl, 0.2 mM KC1, 0.8 mM Na_2HP0_4, 0.2 mM KH_2P0_4, pH 7.4. Fluka Chemicals, Buchs, Switzerland) and fixed in a 4% paraformaldehyde solution (freshly prepared from a 20% stock solution, paraformaldehyde powder from Fluka Chemicals, Buchs, Switzerland) for 1 hour. After rinsing with PBS, the cells were permeabilized using 0.5% Triton X-100 (Fluka Chemicals, Buchs, Switzerland) for 15min at room temperature followed by three rinses with PBS. The nucleus was stained with DAPI (4',6-diamidino-2-phenylindole, 1:1000 dilution in PBS; Invitrogen, Basel, Switzerland) for 30 min at room temperature. The substrata were rinsed again with PBS and kept in PBS to prevent them from drying.

6.1.3.3 Experimental design for attachment test II

Experimental design II was similar to experimental design I, except that this time coating was applied to titanium disks, to assess whether cell attachment would be similar than to the coated glass slides.

Group 1: Tissue culture glass
Group 2: Fluoroalkylsilane coated Ti-A-S
Group 3: Silica coated Ti-A-S
Group 4: Both silica and fluoroalkylsilane coatings (superhydrohobic) on Ti-A-S

Cleaned Ti-A-S surfaces were used for the coatings. Experiment was performed according to the same protocol as the one described in 6.4.2., except only fluorescence microscopy was used to determine the cell numbers and SEM examination of cell morphology was not done.

6.1.3.4 Characterization of cell adhesion

In order to evaluate the nature cell adhesion to the surfaces, analysis of both cell number and cell morphology were performed. Cell number on samples was examined with optical microscope and fluorescent microscope (AxioIMAGER M1m, Zeiss, Oberkochen, Germany) using a DAPI filter set (filter set no. 49 and 10, Zeiss, Oberkochen, Germany) and 20X magnification. Scanning electron microscope (Hitachi 800) was used to examine the cell morphology on the different coatings on glass.

In order to determine the average cell number, 10 images were taken from different locations. Cell numbers were counted manually from the optical images and the nuclei from fluorescence images were counted manually as well as with the help of ImageJ software (Version 1.36b for Mac OS X). The average cell number was calculated for each sample and these averages were used to determine the average cell number for each group. Standard error for each sample and group were calculated similarly.

Prior to SEM examination, samples were dehydrated using graded series of ethanol. 1mL of mixture of ethanol and DI water, starting from 35% of ethanol, was added onto the samples and changed every 12h to 15% higher concentration until 100% ethanol was reached. Samples were let dry in ambient air for 30min before a thin layer of gold was sputter-coated (Ernest F. Fullam Inc, EFFA® Carbon Coater and Sputter Coater) onto them prior to SEM examination.

6.1.4 Toxicity evaluation of the coatings

If the superhydrophobic coating were to be used in medical implants, it should not have any adverse effects on cell viability. To evaluate the possible toxicity of the coating, MTT assay test was performed.

6.1.4.1 Working principle of the MTT assay

The MTT test is a colorimetric assay which measures the reduction of a tetrazolium component (MTT, 3-(4,5-Dimethylthiasol-2-yl)-2,5-diphenyltetrazolium bromide) into an insoluble purple formazan product by the mitochondria of viable cells. It can be used to determine the cytotoxicity of potential medical agents and other materials since released agents would result in cell toxicity and therefore metabolic dysfunction and decreased performance in the assay. [187]

6.1.4.2 Performing the assay

After incubating the cells with the MTT reagent for approximately 2 to 4 hours, a detergent solution (dimethyl sulfoxide or acidified ethanol solution) is added to lyse the cells and solubilize the colored formazan crystals. The samples are read using a spectrophotometer at a wavelength of 570 nm. The amount of color produced is directly proportional to the number of viable cells and comparisons between the spectra of treated and untreated cells can give a relative estimation of cytotoxicity. [187]

6.1.4.3 Experimental design for MTT toxicity test

Purpose of this experiment was to evaluate whether the original superhydrophobic coating and the PDMS modified version are toxic to MG63 cells.

Group 1: Full media (FMOB)
Group 2: Conditioned media - Tissue culture glass
Group 3: Conditioned media - Fluoroalkylsilane coated glass
Group 4: Conditioned media - Silica coated glass
Group 5: Conditioned media - Silica coating modified with (PDMS) on glass
Group 6: Conditioned media - Both coatings 3&4 (superhydrohobic) on glass

The superhydrophobic samples in group 5 have two coatings, one to create surface roughness (thin film composed of silica particles, group 3) and another one to lower the surface energy (monolayer of fluoroalkylsilane, group 2). Coating in group 4 is a modification of group 3 (for improving the mechanical properties of the original coating).

Samples (3 per treatment) were put into 12-well plate and incubated with 1mL FMOB for 48h. Media was then collected and surfaces incubated with 1mL of FMOB for additional 24h which was then collected and combined with the previously acquired media. MG63 cells were plated into 24 well plates and 24h after plating either FMOB or conditioned media was used to feed confluent cultures (0.5mL/well). Cells were be harvested at day 3 and 5 and at harvest media was replaced with FMOB.

20h after the media was changed, 10uL of MTT dye was added to each well and cells were incubated for an additional 4h. After this, cells were rinsed two times with PBS and 200uL of DMSO was added to each well. Plates were rocked for 30 minutes to allow the crystals to dissolve and solution was read in a 96 well plate using the Benchmark plate reader.

6.2 Results and discussion

Contact angle measurements were done to evaluate the wetting of the prepared surfaces. Scanning electron microscopy and atomic force microscopy (AFM, tapping mode) were used to characterize the surface morphology and structure of the thin films. X-ray photo electron spectroscopy (was conducted to verify the chemical composition of the coatings. The effect of adding PDMS on coating chemistry and morphology is also reported.

Cell number on the on the samples was determined using optical and fluorescence microscopy and this data was used to evaluate cell adhesion onto the surfaces. Cell morphology was examined with scanning electron microscopy to see whether the attached cells appeared viable. Results from the MTT assay are presented and coating toxicity evaluated based on them. Biological experiments were conducted twice and the data shown are from one representative experiment.

6.2.1 Surface wettability

Silica films without fluoroalkylsilane layer displayed very low contact angles and coatings can thus be said to be superhydrophilic. Fluoroalkylsilane treated smooth glass displayed average contact angle of 106°. Higher contact angles, closer to the theoretical maximum of 120° were obtained later with longer exposure times in the UV-ozone cleaner prior to treatment, but these surfaces were not used in cell culture experiments. Fluoroalkylsilane treated Ti-A-S disks displayed higher contact angles close to the superhydrophobic regime, because they already had some surface roughness on them. This roughness was however mostly in the micron scale so applying the sol-gel coating to the disks, resulted in both nano- and micron scale surface features and superhydrophobicity together with fluoroalkylsilane treatment. Contact angles of the superhydrophobic films (Figure 16) on were slightly lower than on titanium which was most probably due to better coating adhesion and uniformity on metal. Average readings for all the different coatings were reported (Table 1, Figure 17). Contact angle hysteresis of the superhydrophobic surfaces was below 10° and water rolled off them easily.

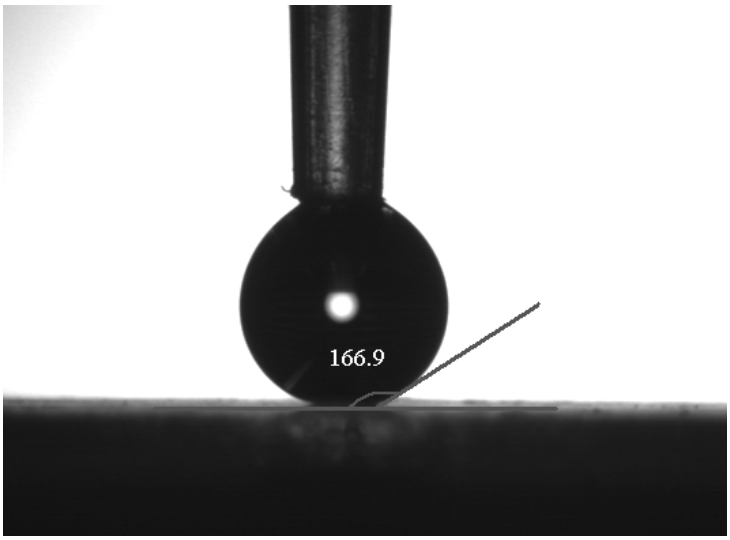

Figure 16 Water droplet on the superhydrophobic coating (166.9°)

On the PDMS modified coatings water contact angles of over 160° and contact angle hysteresis lower than 10°, and thus superhydrophobicity were also was achieved. Coatings silica coatings prepared by dip coating, instead of spinning the sol on them were superhydrophobic as well (after fluoroalkylsilane treatment), and displayed relatively good film uniformity. Better quality coatings will surely be obtained with proper dip coating equipment.

Table 1 Average contact angles on different coatings

Group	Mean	Std Error
1. Glass	50.887	20.774
2. Fluoroalkylsilane (coating 2) on glass	106.483	43.472
3. Silica (coating 1) on glass	7.477	3.052
4. Fluoroalkylsilane (coating 2) on titanium	131.437	53.659
5. Silica (coating 1) on titanium	6.147	2.509
6. Superhydrophobic (coatings 1+2) on glass	164.797	67.278
7. Superhydrophobic (coatings 1+2) on titanium	167.043	68.195

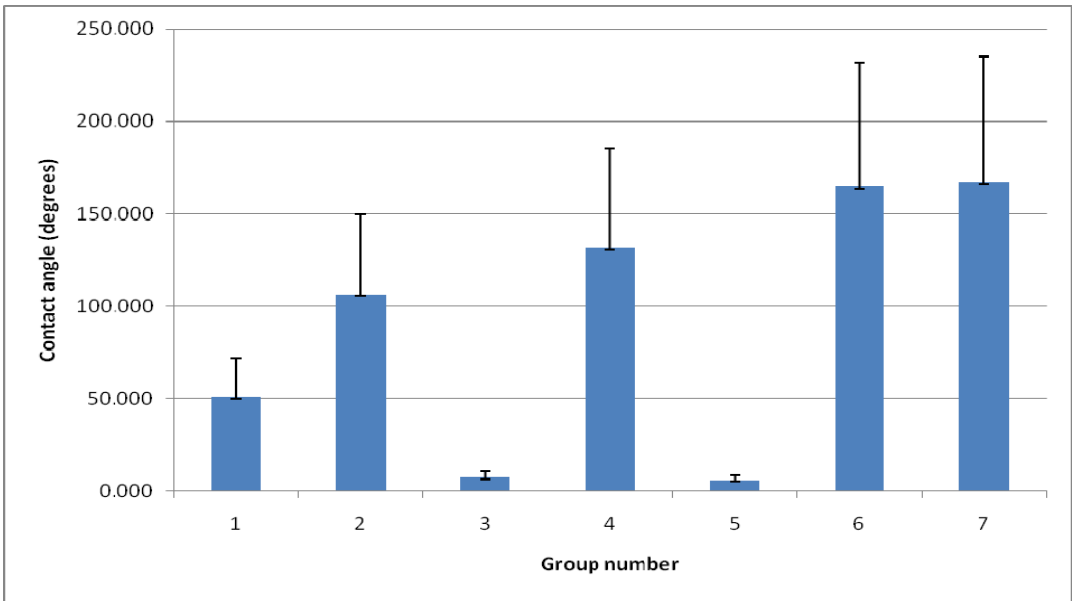

Figure 17 Average contact angles on different coatings

Taking θ = 110° and θ* = 165° eq. (3) can be used to estimate a f value of 0.052 which suggests that approximately 5% of the surface of a drop will effectively be in contact the surface. Thus, the hypothesis is that this feature could have implications when a solid

substrate is in contact with biological elements suspended in a liquid medium, including cells or proteins [14].

6.2.2 Surface morphology

The preparation of superhydrophobic surfaces requires controlling the surface roughness. Using eutectic liquid as a solvent and a templating agent in the sol-gel process creates rough microstructures. Ethanol evaporates from the solution during spin coating, but the eutectic liquid remains and prevents the porous structure from collapsing. After gelation and aging for one week eutectic liquid is extracted from the film by rinsing it with ethanol. Film morphology can be described as an aerogel since it retains its original volume whereas a xerogel would show more shrinkage due to reduced porosity caused by capillary forces.

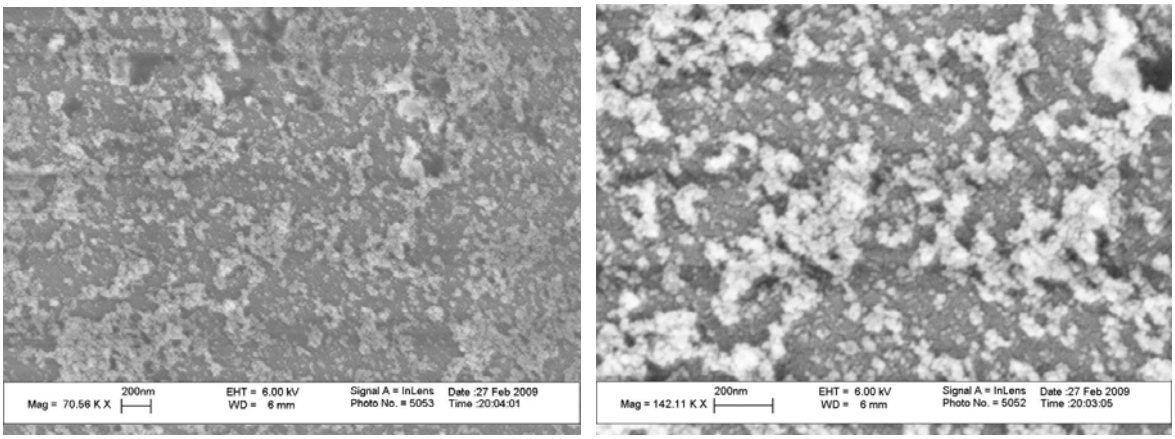

Figure 18 SEM images of the superhydrophobic coating on glass (spin coated)

From SEM images, the silica films creating the roughness for the superhydrophobic surface, seems to consist of clusters of silica particles of 10-30 nm radii. The size scale of these clusters varies from 50 nm to over 200nm. The larger clusters are spaced 100 to 500 nm from each other, while there are smaller clusters in between (Figure 18 and Figure 19). Films do not seem completely uniform which is most likely due to the insufficient cleanliness of the coated surfaces. Though the substrates were carefully cleaned, they were exposed dust and other particles in laboratory air before the coating process could be completed. Dip coated surfaces displayed similar morphology, though slightly denser surface structures (Figure 19), and coating covered the surfaces better compared to spinned coatings (Figure 18).

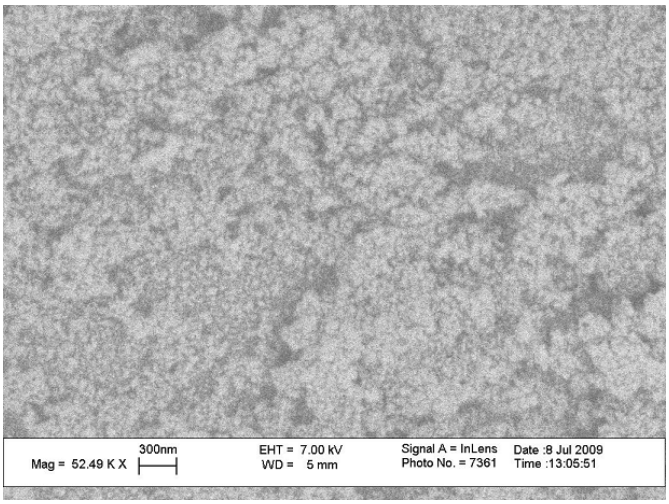

Figure 19 SEM image of the superhydrophobic coating on glass (dip coated)

On the Ti-A-S surfaces, the superhydrophobic coating looks slightly different due to the rougher underlying substrate surface (Figure 20). Silica particles forming the film can still be detected. The uncoated Ti-A-S disks had small pits (2 μm in diameter) and randomly oriented scratches from the polishing operation, which were only evident at high magnification. Profilometry of the disks showed average roughness (R_a) of 1.149-2.211μm, RMS roughness of 1.370-2.472 μm and peak to valley height of 7.525-8.509 μm.

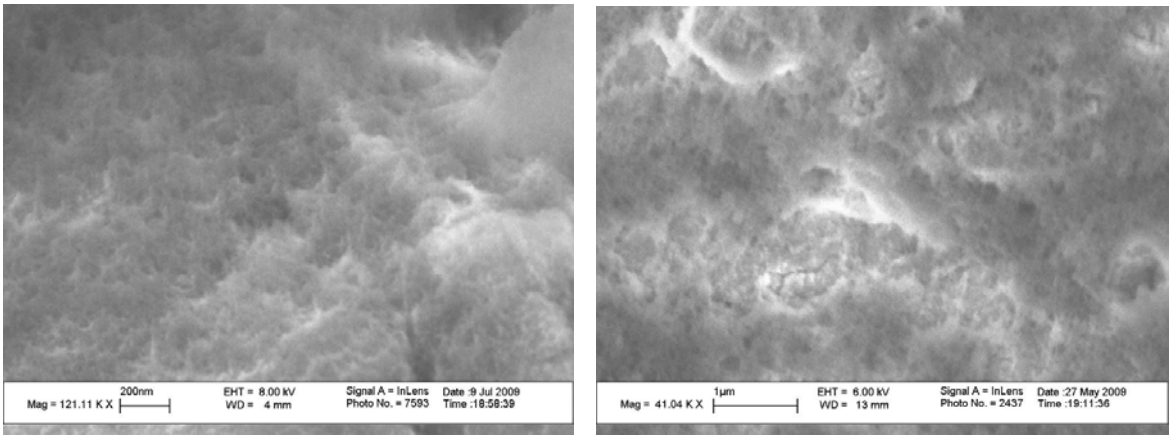

Figure 20 SEM images of the superhydrophobic coating on rough (a) and smooth (b) Ti-A-S surface (spin coated)

Film thickness could be controlled with the amount of ethanol added to the sol as well as with spin speed. Films prepared using 3 g of ethanol (with 2.4g C-U and 0.6g TEOS) did not display superhydrophobicity, most likely because they were too thin to have adequate

surface roughness. Due to the amorphous nature of the silica film and the glass slide, film thickness was hard to determine from the SEM cross sectional image, but the film in Figure 21 SEM image of the film cross section seems to be around 400nm.

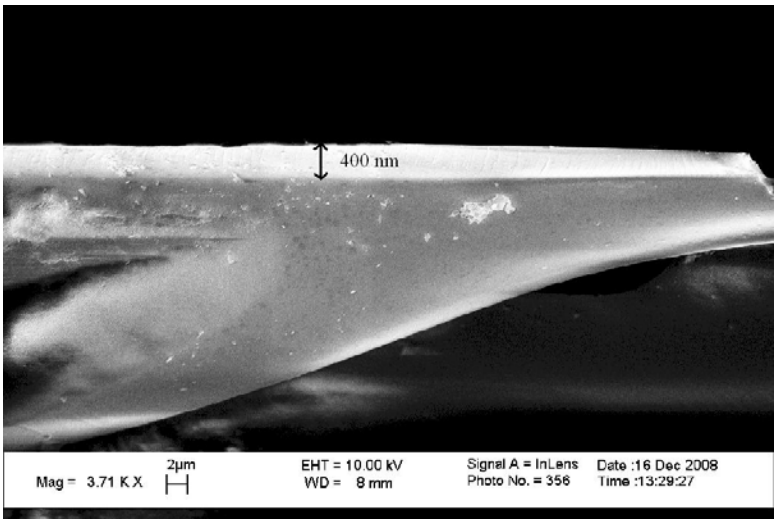

Figure 21 SEM image of the film cross section

SEM images were also recorded on the coatings with different weight percentages (20, 30 and 40wt%) of PDMS (Figure 22). Size of the particles, or clusters of particles, forming the film seems to increase with increasing the amount of PDMS. Also the clusters of particles have more empty space between them which creates more pronounced roughness on the micron level. Hybrid coatings with 40wt% PDMS displayed the highest contact angels which might be due to this increased roughness compared to the coatings with lesser amounts of PDMS.

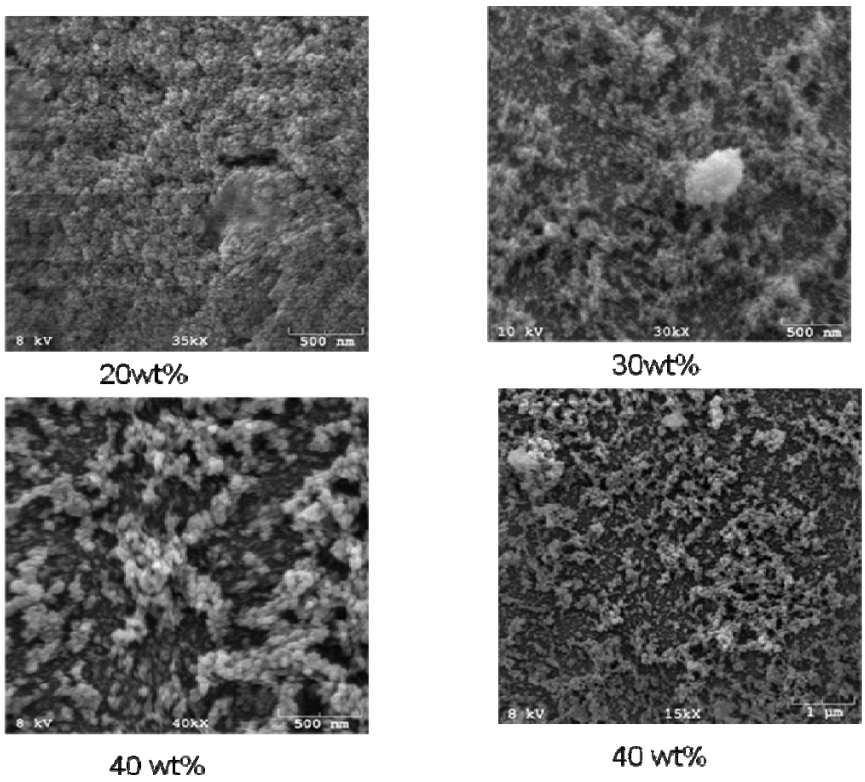

Figure 22 SEM images of TEOS-PDMS hybrid coatings with different weight percentages of PDMS

AFM supports the findings from SEM, also showing silica particles with radii ranging from 10 to 30 nanometers as well as clusters of these particles (Figure 23 and Figure 24). Average surface roughness (Ra) after fluoroalkylsilane treatment was ~49nm. Large scale surface roughness is due to the pores generated by evaporation of solvents (eutectic liquid and ethanol). An additional smaller scale roughness is caused primarily by the silica particle size. Comparing AFM images of the fluoroalkylsilane treated and non-treated films showed protrusions consisted of much finer-scaled roughness attributed to the silane coating.

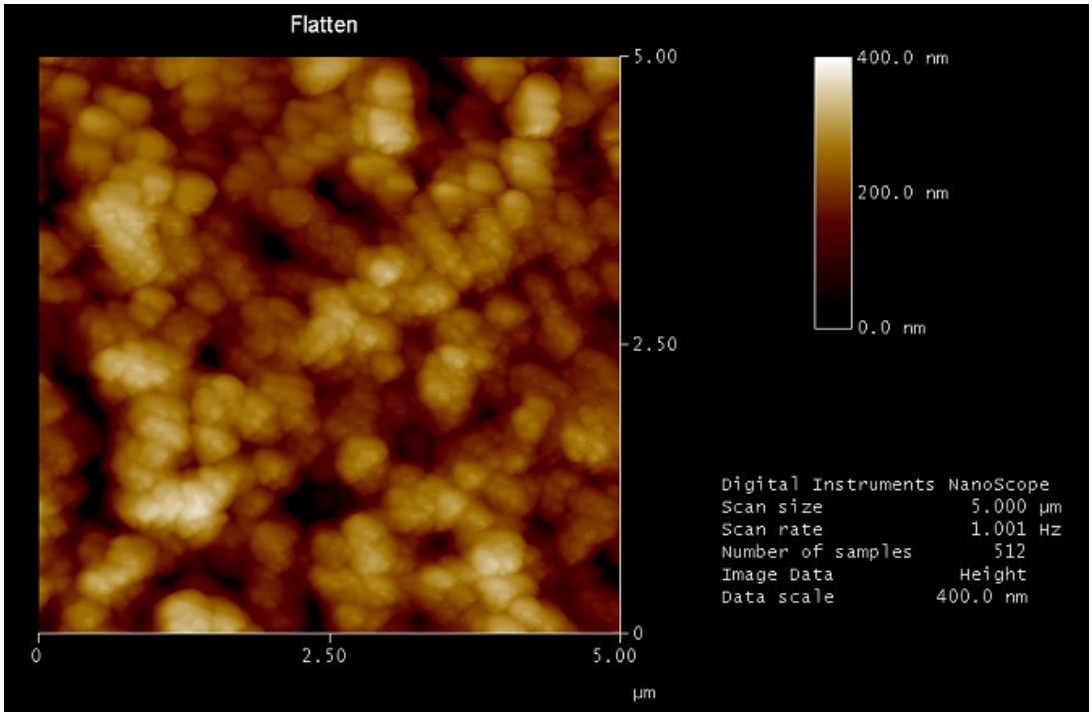

Figure 23 AFM image of the superhydrophobic coating on glass

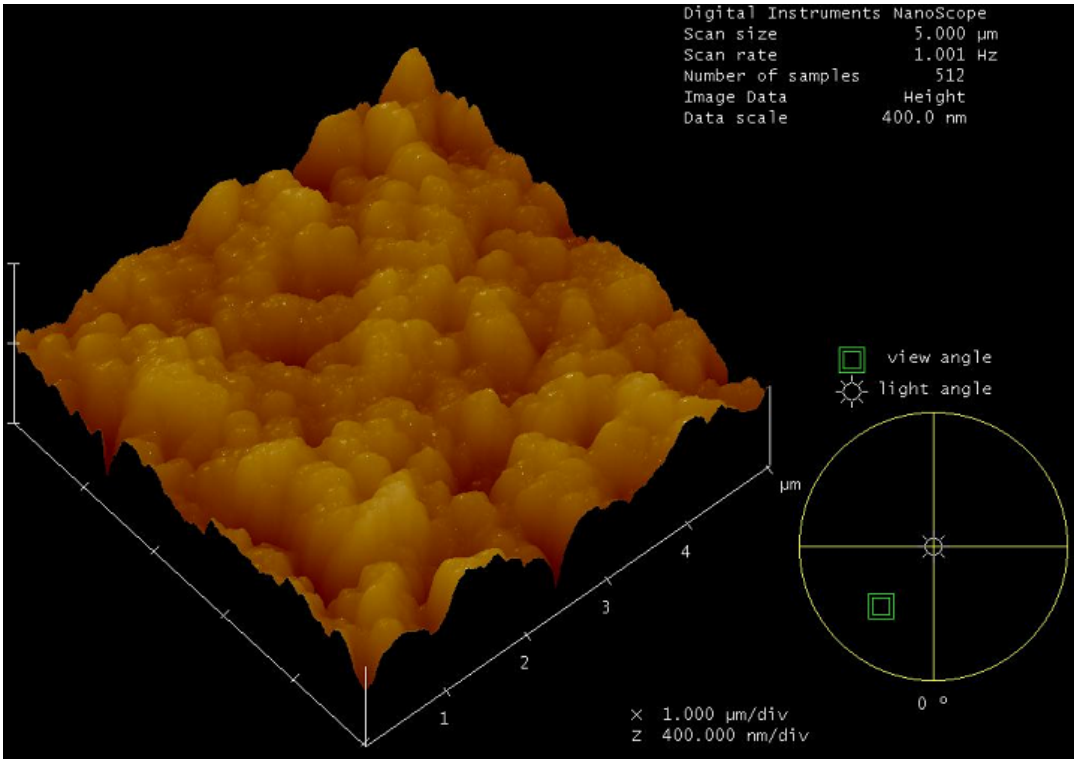

Figure 24 3D presentation of the superhydrophobic surface

6.2.3 Surface chemistry

From the XPS survey of spin coated films, it was found the surface has four elements. The main peaks occur at kinetic energies of 685, 529, 288 and 99 eV. F and C were from the fluorosilane coating, and O and Si from both of the coating and silica film (Figure 25 XPS spectra of superhydrophobic surface). The analysis also performed on the) silane treated glass, silica films and PDMS modified and silane treated films (superhydrophobic). The elemental composition of the different coatings is presented in Table 2. It should be noticed that XPS characterization was performed in vacuum, and that changes in the surface chemistry could be altered when the substrates are put in contact with a liquid, such as water or culture medium.

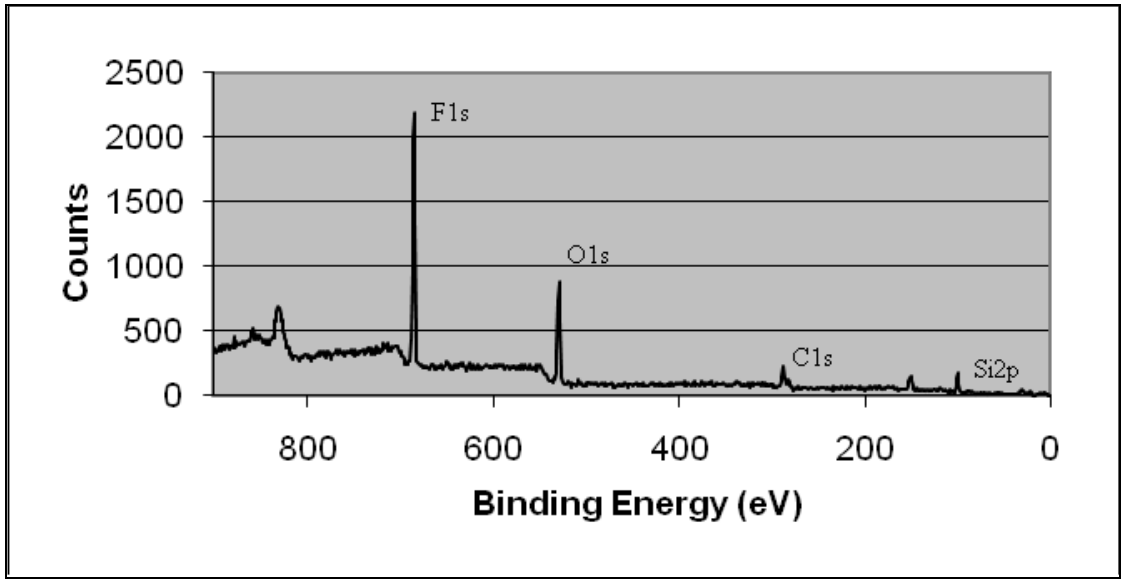

Figure 25 XPS spectra of superhydrophobic surface

Table 2 Elemental composition of the coatings

Elemental %	F 1s	O 1s	C 1s	Si 2p
Superhydrophobic film (silica+silane)	28.297	39.217	19.186	13.3
Superhydrophobic film, PDMS modified silica	32.063	35.033	18.893	14.011
Silica film	0	52.572	27.764	19.664
Silane treated glass	29.718	36.14	19.639	14.503

6.2.4 Cell adhesion

Tissue culture polystyrene (TCPS) could only be examined under a light microscope, whereas the cell number on the silica coating and on the superhydrophobic coating could not be reliably determined with optical microscope due to the surface features. Thus, the optical/fluorescence microscopy data on these groups is not available. As expected, optical microscopy showed less cells on the fluoroalkylsilane coated glass compared to uncoated glass and TCPS (Figure 26 and Figure 27). This can be attributed to the lower surface energy (higher water contact angle) of the coating.

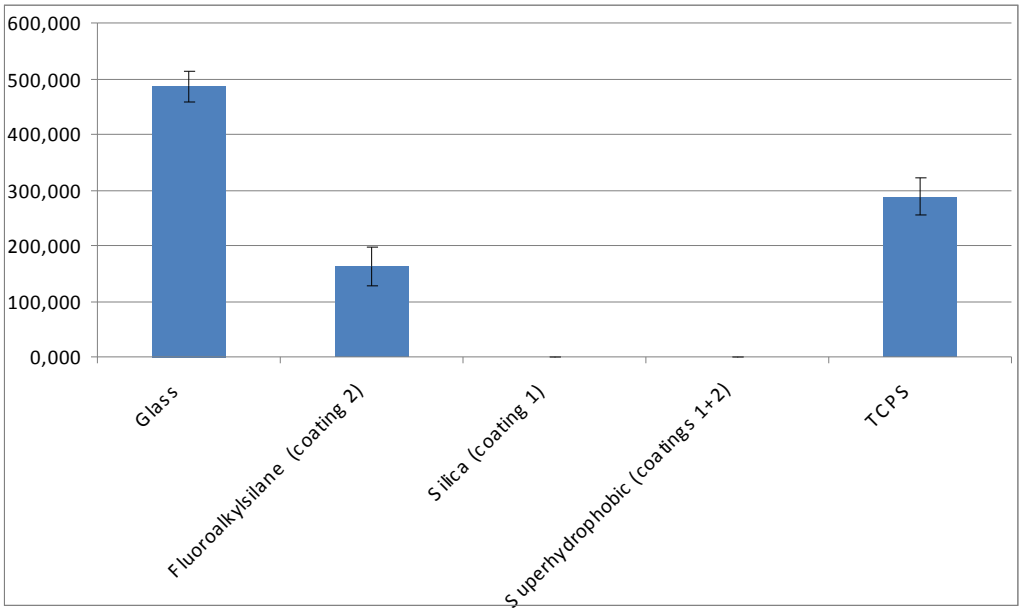

Figure 26 Cell numbers on coated glass detected with optical microscopy

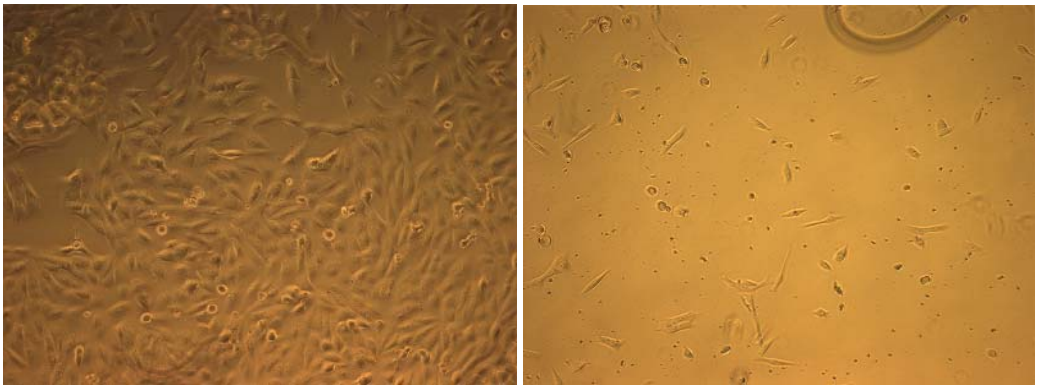

Figure 27 Optical images of MG63 cells on glass (a) and fluoroalkylsilane coated glass (b) after 24h culture

From the fluorescence microscopy, it could be verified that the fluoroalkylsilane coating alone and the superhydrophobic coating both decreased the number of attached cells, though fluoroalkylsilane to lesser extent (Figure 28 and Figure 29). Though the superhydrophobic coating on glass displayed lower cell numbers, some cells could be observed after the first experiment. These cells were mostly found in clusters (Figure 29a) implying that the silica coating was not uniformly covering the substrate. Few changes were made to the sol (addition of P123 and reducing the amount of ethanol from 2.5 g to 2 g) and in the repeat experiment such clusters of cells could not be observed (Figure 29b). Cell numbers based on fluorescence microscopy are presented in Figure 30

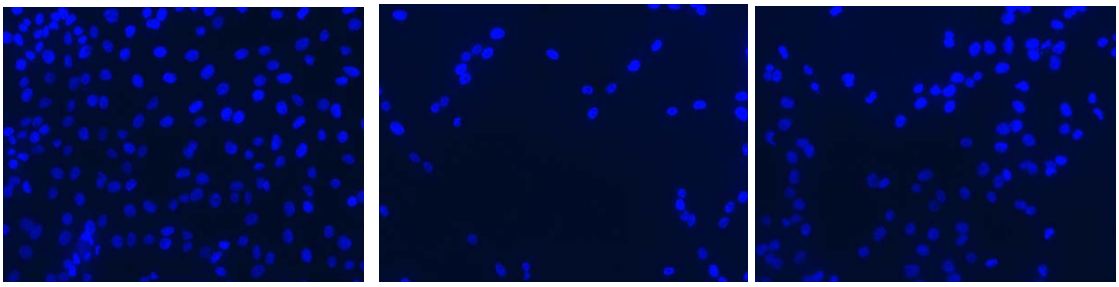

Figure 28 Fluorescence microscopy images of glass (a), fluoroalkylsilane coated glass (b) and silica coated glass (c) after 24h hours of culture

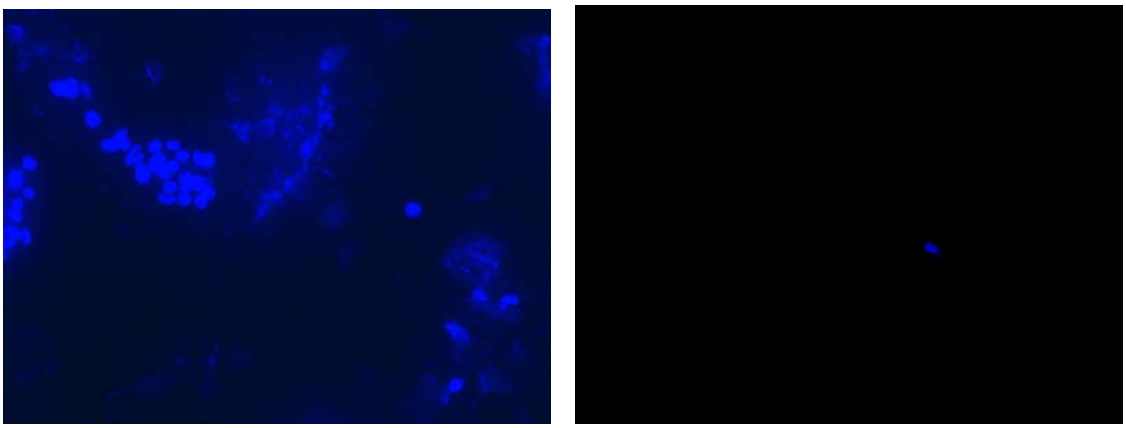

Figure 29 Fluorescence microscope image of cells on the superhydrophobic coating on glass, after the first experiment (a) and the repeat experiment (b)

Superhydrophobic surfaces and the fluoroalkylsilane coated glass had the same low energy surface chemistry so the decreased cell numbers on the superhydrophobic surfaces are caused by underlying surface roughness. The air trapped in the surface features limits the contact of culture media and the cells with the surface, making them unable to adhere to it.

Surface roughness alone did not prevent cell adhesion when the chemical surface energy was not low (sol-gel silica coating without fluoroalkylsilane).

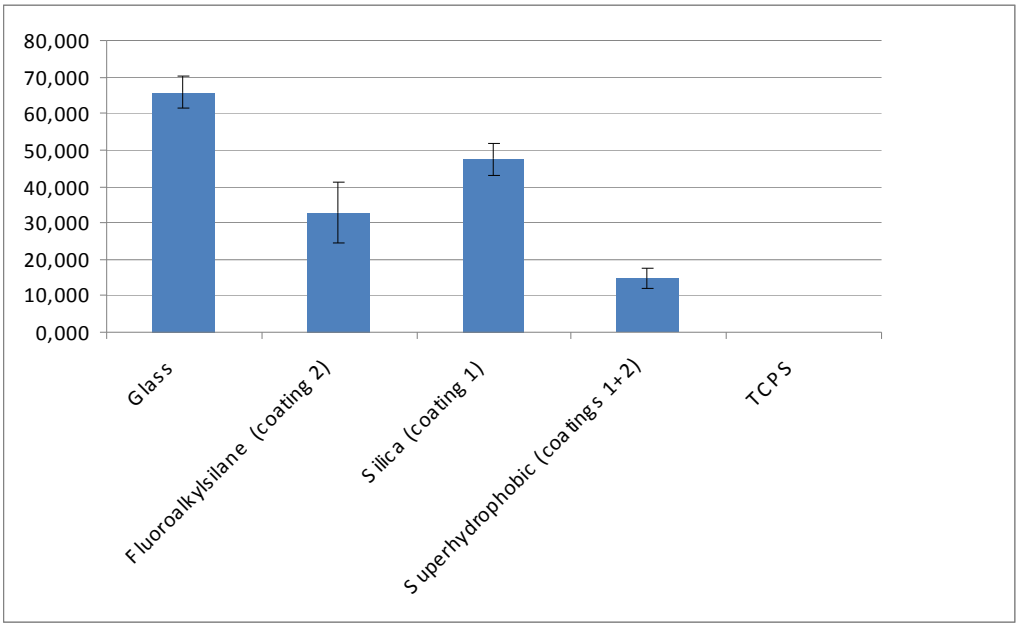

Figure 30 Cell numbers on coated glass from fluorescence microscopy

Similar results were also obtained with the coated Ti-A-S surfaces. Superhydrophobic coating displayed the lowest cell numbers and the fluoroalkylsilane coating decreased cell attachment compared to glass control surfaces. On rough Ti-A-S surfaces, sol-gel silica coating displayed an increased number of attached cells compared to glass. Unfortunately uncoated Ti-A-S disks were not used as a control, so it could not be concluded whether the silica coating would increase cell number compared to the uncoated surface. Cell numbers on coated Ti-A-S are shown in Figure 31.

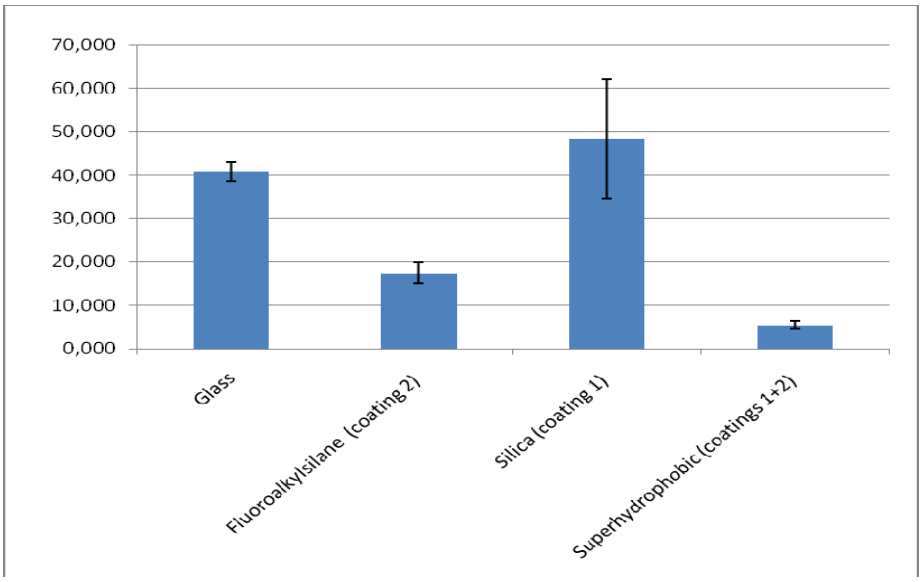

Figure 31 Cell numbers on coated Ti-A-S

Cell adhesion data from both coated glass (repeat experiment performed simultaneously with the experiment using Ti-A-S disks) and Ti-A-S are presented in Table 3 and Figure 32 Summary of the cell numbers on both coated glass and Ti-A-S (fluorescence microscopy). Though superhydrophobic coating on titanium displayed higher contact angles compared to coated glass, cell adhesion to cell adhesion to it was slightly greater. The same could be observed with the two substrates with the fluoroalkylsilane coating alone. This increase in cell adhesion is most likely due to the micron scale roughness of the titanium disks since roughness has been previously reported to enhance osteoblast adhesion, especially when in the micrometer range [186].

Group	Mean	SEM
1.Glass	40,746	2,121
2. Fluoroalkylsilane (coating 2) on glass	9,817	2,401
3. Silica (coating 1) on glass	21,850	3,909
4. Fluoroalkylsilane (coating 2) on Ti-A-S	17,450	2,350
5. Silica (coating 1) on Ti-A-S	48,350	13,752
6. Superhydrophobic (coatings 1+2) on glass	2,950	0,555
7. Superhydrophobic (coatings 1+2) on Ti-A-S	5,478	0,902

Table 3 Summary of the cell numbers on both coated glass and Ti-A-S (fluorescence microscopy)

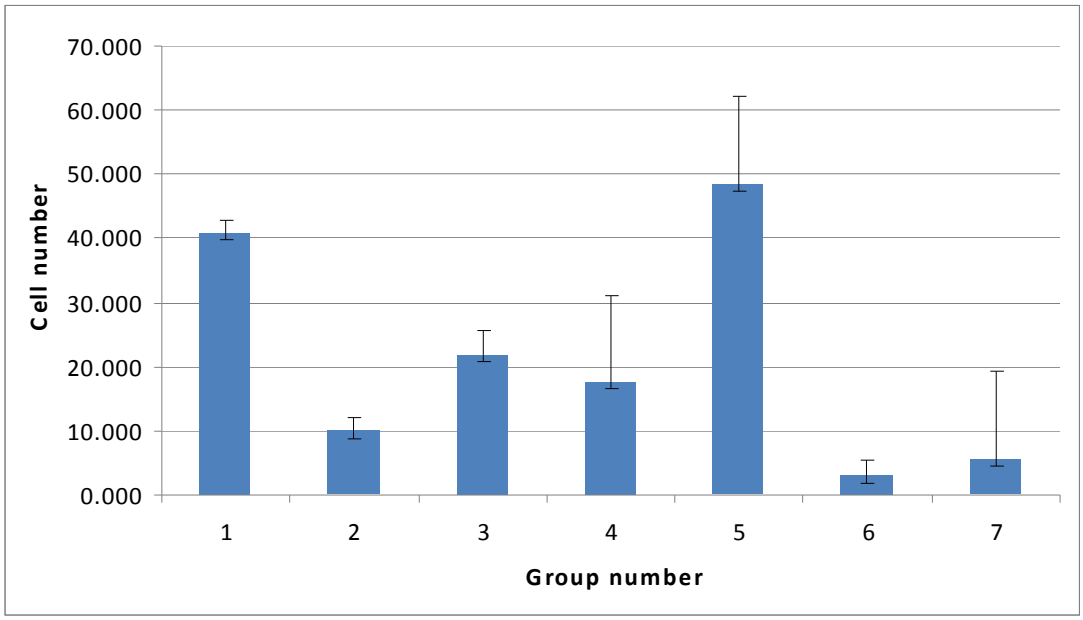

Figure 32 Summary of the cell numbers on both coated glass and Ti-A-S (fluorescence microscopy)

6.2.5 Cell morphology

Cells on fluoroalkylsilane and silica coatings displayed similar elongated morphologies than on glass (Figure 33), fluoroalkylsilane coating (Figure 34) and silica coating (Figure 35) implying the adhered cells were normal and non-necrotic. No cells could be observed on the superhydrophobic surfaces supporting the fluorescence microscopy data on reduced cell attachment, though this might also be partially because the surface roughness makes detecting cells difficult (Figure 36).

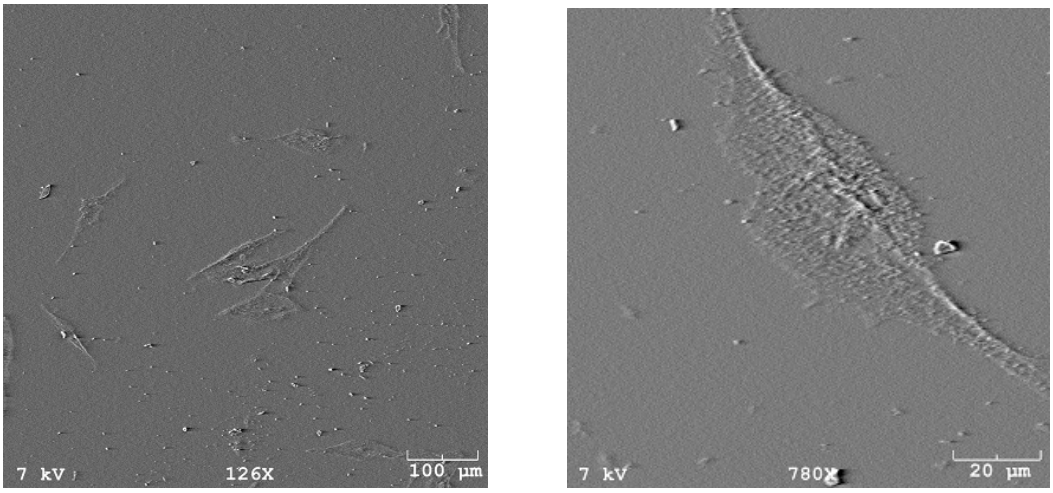

Figure 33 MG63 cells on a glass surface after 24h culture period

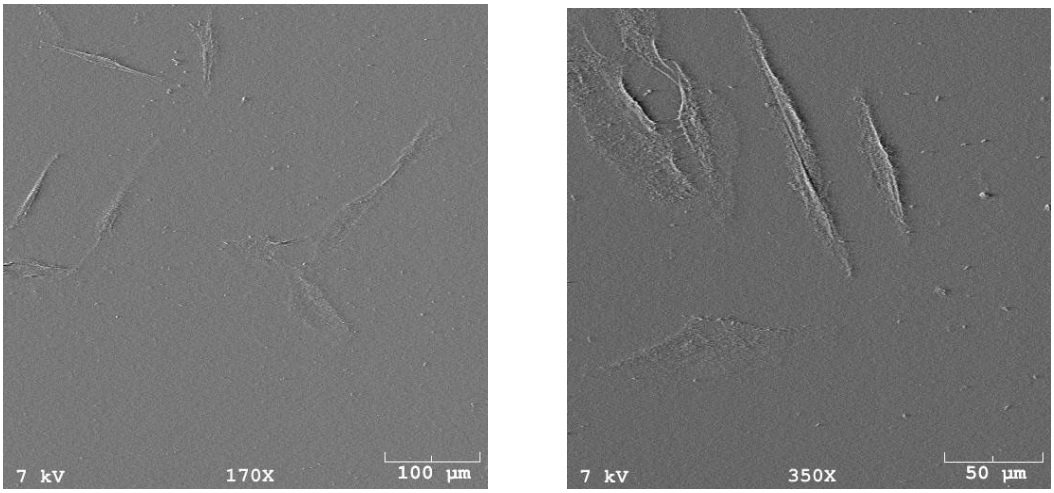

Figure 34 SEM images of MG63 cells on Fluoroalkylsilane treated glass after 24h culture period

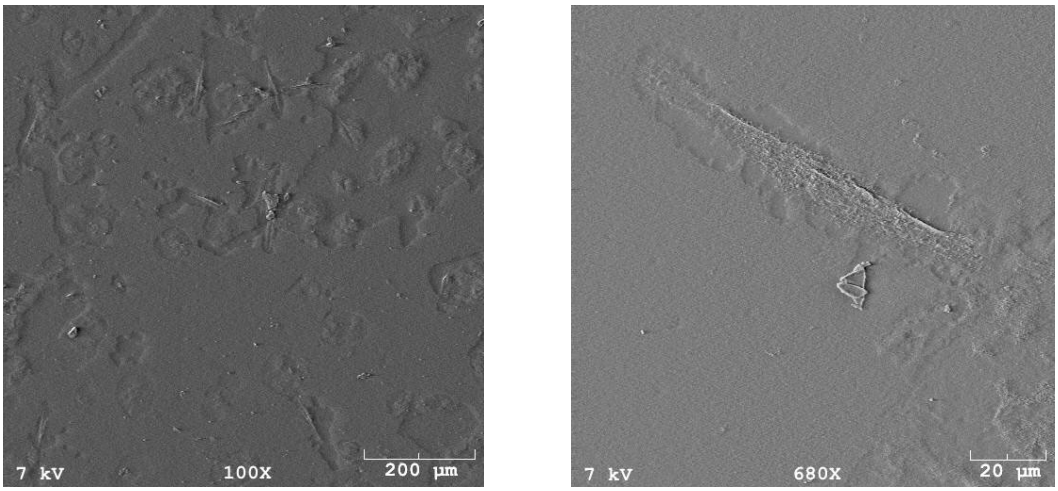

Figure 35 SEM images of MG63 cells on silica coated glass after 24h culture period

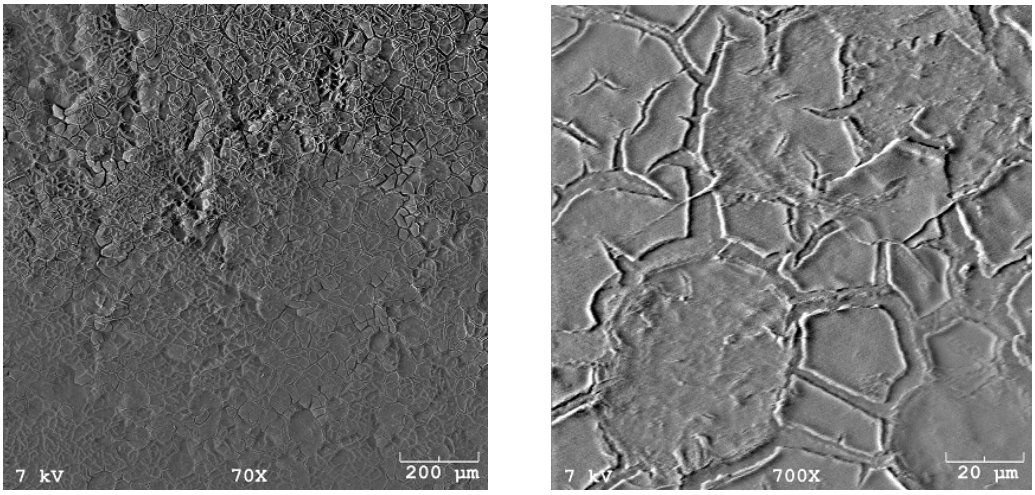

Figure 36 SEM images of the superhydrophobic coating with no visible cells after 24h culture period

6.2.6 Cell viability on the coatings

Based on the previously published literature, none of the individual coatings should be cytotoxic. Also, cells founds on the surfaces in the attachment experience seemed normal though their number was lower than on glass. MTT assay showed little difference in cell viability on different coatings (Figure 37).

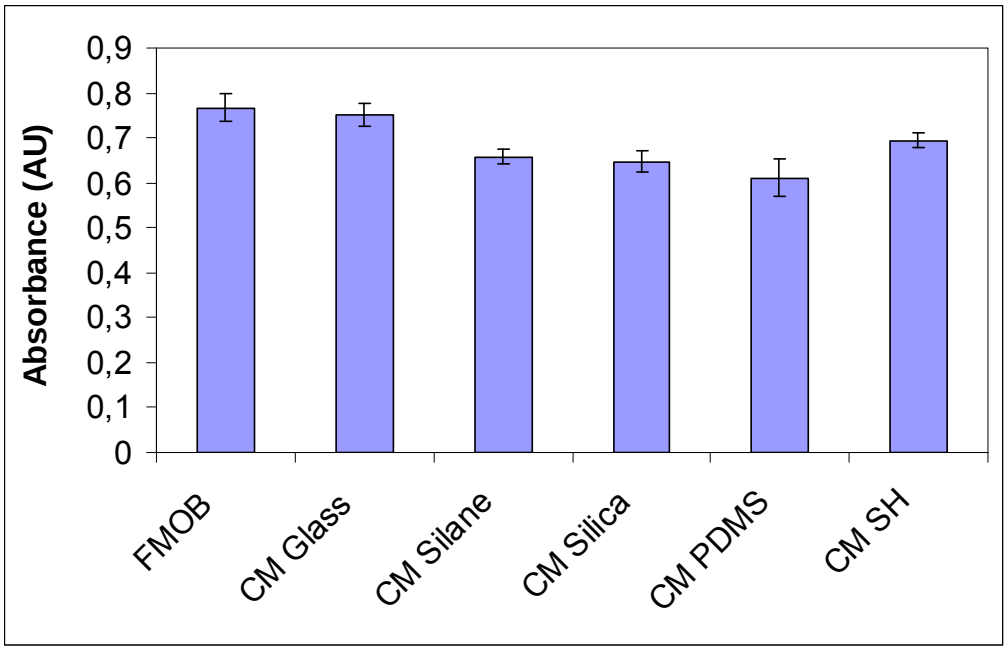

Figure 37 Results from MTT assay after day 3

6.3 Conclusion

In this master's thesis, superhydrophobic coatings were prepared using sol-gel technology in combination with fluoroalkylsilane coating. Surface characteristics of the coatings were also reported. Preliminary tests focusing cell viability, adhesion and proliferation of cells were performed as well, in order to demonstrate the effect of superhydrophobicity on the behavior of mammalian cells and to evaluate the potential of the superhydrophobic coating for preventing unwanted bioadhesion in medical implants, such as catheters and biosensors. Superhydrophobic coating was demonstrated to have the ability to resist cell adhesion.

Superhydrophobic surfaces can be prepared in variety of different ways, but for the use biomedical applications certain criteria, such as non toxicity, must be met. The combination of sol-gel technology with a low surface energy fluoroalkylsilane coating applied in the biological setting in this thesis is suitable for biomedical applications. Preparation of the coating is easy and it can be applied on different substrate materials and geometries via dip coating. Coating process does not require any specific equipment compared to the several methods achieving superhydrophobicity with surface modifications, such as plasma treatments. The resulting coating is also chemically stable and non-toxic.

Incorporating PDMS to the silica coating was also successful in terms of creating suitable surface features for achieving superhydrophobicity, but the effect of this modification on the mechanical properties of the coating was not quantified. In preliminary bending tests, aluminum foils with the hybrid coating seemed to tolerate bending better, compared to the unmodified silica coating, when it came to the coating appearance and contact angles on the coating before and after bending.

Long term performance of the coating when exposed cell culture and physiological conditions was not investigated, and it has been suggested that the antifouling effect caused by surface superhydrophobicity would be lost in underwater conditions in the long run [157]. Applicability of this coating on different biomaterials, namely polymers, was also not investigated. In conclusion, based on the preliminary cell adhesion and toxicity tests, this superhydrophobic coating has potential for coating medical implants in instances where cell and bacterial adhesion is not desired, but further studies would have to be conducted if it were to be used in actual medical applications. Testing the coating's performance when exposed to oral bacterial environment is currently underway.

7 References

1 D. Öner and T. J. McCarthy, Ultrahydrophobic surfaces. Effects of topography length scales on wettability, Langmuir 2000;165:7777–7782

2 K. Ino, A. Ito, Y. Wu, N. Saito, E. Hibino, O. Takai, and H. Honda, Application of Ultra-Water-Repellent Surface to Cell Culture, Journal of Bioscience and Bioengineering 2007;104(5):420–423

3 X. J. Feng and L. Jiang, Design and creation of superwetting/antiwetting surfaces, Advanced Materials 2006;18(23):3063–3078

4 A.B. D Cassie and S. Baxter, Large contact angles of plant and animal surfaces, Nature 1945;155:21–22

5 E. A. Baker, Chemistry and morphology of plant epicuticular waxes, In: D.F. Cutler, K. L. Alvin and C.E. Price (eds) The plant cuticle. Academic Press, London 1982; 139-166

6 W. Barthlott and C. Neinhuis, Purity of the sacred Lotus, or escape from contamination in biological surfaces, Planta 1997;202(1):1-8

7 Y. Cheng, D. Rodak, A. Angelopoulos and T. Gacek, Microscopic observations of condensation of water on lotus leaves, Applied Physics Letters 2005;87

8 D. Quere, Wetting and Roughness, Annual Review of Materials Research 2008:38;71-99

9 J. M. Anderson, A. Rodrigugez and D. T. Chang, Foreign body reaction to biomaterials, Seminars in Immunology 2008;20(2):86-100

10 K. R. Patel, H. Tang, W. E. Grever, K. Y. Simon Ng, J. Xiang, R. F. Keep, T. Cao and J. P. McAllister II, Evaluation of polymer and self-assembled monolayer coated silicone surfaces to reduce neural cell growth, Biomaterials 2006;27:1519–1526

11 J. Lee, B.S. Kang, B. Hicks, T. F. Chancellor Jr., B. Hwan Chu a, H. Wang, B. G. Keselowsky, F. Rena and T. P. Lele, The control of cell adhesion and viability by zinc oxide nanorods, Biomaterials 2008;29:3743-3749

12 C. Mao, Y. Qiu, H. Sang, H. Mei, A. Zhu, J. Shen and S. Lin, Various approaches to modify biomaterial surfaces for improving biocompatibility, Advanced Colloid Interface Science 2004;110:5–17

13 H. Thissen, G. Johnson, P. G. Hartley, P. Kingshott and H. J. Griesser, Two-dimensional patterning of thin coatings for the control of tissue outgrowth, Biomaterials 2006;27:35–43

14 N. M. Alves, J. Shi, E. Oramas, J. L. Santos, H. Tomás and J. F. Mano, Bioinspired superhydrophobic poly(L-lactic acid) surfaces control bone marrow derived cells adhesion and proliferation, Journal of Biomedical Materials Research Part A Published Online: 4 Nov 2008

15 A.Okada, T.Nikaido, M. Ikeda, K. Okada, J. Yamauchi, R. M. Foxton, H. Sawada, J. Tagami and K. Matin, Inhibition of Biofilm Formation using Newly Developed Coating Materials with Self-cleaning Properties, Dental Materials Journal 2008;27(4):565-572

16 H. Tang, T. Cao, A. Wang, X. Liang, S. O. Salley, J. P. McAllister II and K. Y. Simon Ng, Effect of surface modification of silicone on Staphylococcus epidermidis adhesion and colonization, Journal of Biomedical Materials Research Part A (2007) DOI 10.1002/jbm.a
17 N. Wisniewski and M. Reichert, Methods for reducing biosensor membrane biofouling, Colloids and Surfaces B: Biointerfaces 2000;18:197–219
18 G. J. Shah and M. Sit, Modeling and Design of Biomimetic Adhesives Inspired by Gecko Foot-Hairs**,** Robotics and Biomimetics 2004, ROBIO 2004, IEEE International Conference
19 M. Nosonovsky and B. Bhushan, Roughness-induced superhydrophobicity: a way to design non-adhesive surfaces, Journal of Physics: Condensed Matter 2008; 20
20 ramé-hart website http://www.ramehart.com/goniometers/contactangle.htm
21 T. Young, An essay on the cohesion of fluids, Philosophical Transactions of the Royal Society of London 1805;A 95:65–87
22 E.G. Shafrin and W.A. Zisman, Upper limits to the contact angles of liquids on solids. In Contact Angle, Wettability and Adhesion: Advances in Chemistry Series 1964;43:145–157
23 N.A. Patankar, On the modelling of hydrophobic contact angles on rough surfaces, Langmuir 2003;19:1249-1253
24 A. Marmur, Wetting on hydrophobic rough surfaces: to be heterogeneous or not to be?, Langmuir 2003;19:8343-8348
25 A. Lafuma and D. Quere, Superhydrophobic states, Nature Materials 2003:2;457-460
26 A. J. Schraut and N. P. Suh, Axiomatic Design of Non-Wetting Hemocompatible Surfaces, Proceedings of ICAD 2006, 4th International Conference of Axiomatic Design
27 R. N. Wenzel, Resistance of solid surfaces to wetting by water. Industrial and Engineering Chemistry 1936;28:988–994
28 A. Marmur, Underwater superhydrophobicity: theoretical feasibility, Langmuir 2006;22:1400-1402
29 X. Li, D. Reinhoudt and M. Crego-Calama, What do we need for a superhydrophobic surface? A review on the recent progress in the preparation of superhydrophobic surfaces, Chemical Socoety Reviews 2007;36:1350–1368
30 B. He, N. A. Patankar and J. Lee, Multiple Equilibrium Droplet Shapes and Design Criterion for Rough Hydrophobic Surfaces, Langmuir 2003;19:4999-5003
31 R. Furstner, W. Barthlott, C. Neinhuis and P. Walzel, Wetting and Self-Cleaning Properties of Artificial Superhydrophobic Surfaces, Langmuir 2005:21;956-961
32 Z. Yoshimitsu, A. Nakajima, T. Watanabe and K. Hashimoto, Effects of Surface Structure on the Hydrophobicity and Sliding Behavior of Water Droplets, Langmuir 2002;18:5818-5822
33 J. T. Han, Y. Zheng, J. H. Cho, X. Xu and K. Cho, J. Phys. Chem. B, 2005, 109, 20773
34 M. L. Ma, Y. Mao, M. Gupta, K. K. Gleason and G. C. Rutledge, Superhydrophobic Fabrics Produced by Electrospinning and Chemical Vapor Deposition, Macromolecules 2005;38:9742-9748

35 N. Zhao, F. Shi, Z. Q. Wang and X. Zhang, Combining Layer-by-Layer Assembly with Electrodeposition of Silver Aggregates for Fabricating Superhydrophobic Surfaces, Langmuir 2005;21:4713-4716
36 J. T. Han, Y. Zheng, J. H. Cho, X. Xu and K. Cho, Stable superhydrophobic organic-inorganic hybrid films by electrostatic self-assemply, The Journal of Physical Chemistry B 2005:109(44);773-278
37 G. Zhang, D. Y. Wang, Z. Z. Gu and H. Mohwald, Fabrication of superhydrophobic surfaces from binary colloidal assemply, Langmuir 2005;21:9143-9148
38 T.P. Chou, K. Takahashi, G.Z. Cao, Optically transparent superhydrophobic silica-based films, H.M. Shang, Y. Wang, S.J. Limmer, Thin Solid Films 2005;472:37–43
39 J. T. Han, D. H. Lee, C. Y. Ryu and K. W. Cho, Fabrication of superhydrophobic surface from a supramolecular organosilane with quadruple hydrogen bonding, Journal of American Chemical Society 2004;126(15):4796-4797
40 W. Ming, D. Wu, R. van Benthem and G. de With, Superhydrophobic films from rasberrry-like particles, Nano Letters 2005;5:2298-2301
41 C.J. Brinker, G.W. Scherer, Sol–Gel Science: The Physics and Chemistry of Sol–Gel Processing, Harcourt Brace Jovanovich (Academic Press, Inc.), Boston, 1990.
42 H. Podbieslka and A. Ulatowska-Jarza, Sol-gel technology for biomedical engineering, Bulletin of the Polish Academy of Sciences Technical Sciences 2005;53:261-271
43 R. Gupta and A. Kumar, Bioactive materials for biomedical applications using sol–gel technology, Biomedical Materials 2008;3
44 C. Zolkov, D. Avnir and R. Armon, Tissue-derived cell growth on hybrid sol–gel films, Journal of Materials Chemistry 2004;14:2200–2205
45 S. S. Jedlicka, J. L. McKenzie, S. J. Leavesley, K. M. Little, T. J. Webster, J. P. Robinson, D. E. Nivense and J. L. Rickus, Sol-gel derived materials as substrates for neuronal differentiation: effects of surface features and protein conformation, Journal of Materials Chemistry 2006;16:3221–3230
46 F. Chai, A. Ochsenbein, M. Traisnel, R. Busch, J. Breme and H. F. Hildebrand, Improving endothelial cell adhesion and proliferation on titanium by sol-gel derived oxide coating, Journal of Biomedical Materials Research Part A, Published online: 9 Mar 2009
47 A. C. Pierre and G. M. Pajonk, Chemistry of Aerogels and Their Applications, Chemical Reviews 2002;102(11):4243-4266
48 C. J. Brinkerand and G. W. Scherer, The physics and chemistry of sol-gel processing. Academic Press Inc 1990
49 B. B Mandelbrot, Fractals: Form, Chances and Dimensions; Freeman, San Francisco, 1977
50 http://www.chemat.com/html/solgel.html
51 A. V. Rao, S. D. Bhagat, H. Hirashima, and G. M. Pajonk, Synthesis of flexible silica aerogels using methyltrimethoxysilane (MTMS) precursor, Journal of Colloid and Interface Science 2006;300;279-285
52 A. S. Wells and V. T. Coombe, On the Freshwater Ecotoxicity and Biodegradation Properties of Some Common Ionic Liquids, Organic Process Research &

Development 2006;10:794-798
53 A. P. Abbott, G. Capper, D. L. Davies, R. K. Rasheed, V. Tambyrajah, Novel solvent properties of choline chloride/urea mixtures, Chemical Communications 2003;1:70–71
54 Y. Xiu, D. Hess and C. P. Wong, A Novel Method to Prepare Superhydrophobic, Self-Cleaning and Transparent Coatings for Biomedical Applications, Electronic Components and Technology Conference 2007
55 D.E. Bornside, C.W. Macosko and L.E. Scriven, Spin-coating: One-dimensional model, Journal of Applied Physics 1989;66:5185-5193
56 C.J. Brinker, A.J. Hurd, P.R. Schunk, G.C. Frye and C.S. Ashley, Review of sol-gel thin film formation, Journal of Non-Crystalline Solids 1992;147&148:424-436
57 L.E. Scriven, in: Better Ceramics Through Chemistry III, ed. C.J. Brinker, D.E. Clark and D.R. Ulrich, Mater. Res. Soc. Syrup. Proc., Vol. 121 (Materials Research Society, Pittsburgh, 1988) p. 717.
58 C. Jeffrey Brinker and Alan J. Hurd, Fundamentals of sol-gel dip-coating, Journal de Physique III France 1994;4:1231-1242
59 S. Duoa, M. Li, M. Zhua and Y. Zhou, Polydimethylsiloxane/silica hybrid coatings protecting Kapton from atomic oxygen attack, Materials Chemistry and Physics 2008;112:1093–1098
60 J.D. Mackenzie, Structure and properties of Ormocils, Journal of Sol-Gel Science and Technology 1994;2
61 F. Mammeri, E. Le Bourhis, L. Rozes and C. Sanchez, Mechanical properties of hybrid organic–inorganic materials, Journal of Materials Chemistry 2005;15:3787–3811
62 K. H.Wu, C.M. Chao, T.F. Yeh, T.C. Chang, Thermal stability and corrosion resistance of polysiloxane coatings on 2024-T3 and 6061-T6 aluminum alloy, Surface and Coatings Technology 2007;201:5782-5788
63 S.K. Medda, D. Kundu, G. De, Inorganic–organic hybrid coatings on polycarbonate.: Spectroscopic studies on the simultaneous polymerizations of methacrylate and silica networks, Journal of Non-Crystalline Solids 2003;318:149-156
64 D.P. Dworak, M.D. Soucek, Protective space coatings: a ceramer approach for nanoscale materials, Progress in Organic Coatings 2003;47(3-4):448-457
65 G.W. Critchlow, R.E. Litchfield, I. Sutherland, D.B. Grandy and S. Wilson, A review and comparative study of release coatings for optimised adhesion in resin transfer moulding applications, International Journal of Adhesion and Adhesives 2006;26(8):577-599
66 J. Zuo, P. Keil, M. Valtiner, P. Thissen and G. Grundmeier, Deposition of Ag nanoparticles on fluoroalkylsilane self-assembled monolayers with varying chain length, Surface Science 2008;602(24):3750-3759
67 H. Sugimura, K. Ushivama, A. Hozumi and O. Takai, Lateral force on fluoroalkylsilane self-assembled monolayers dependent on molecular ordering, Journal of Vacuum Science & Technology B 2002;20(1):393-395
68 A. Hozumi and O. Takai, Preparation of ultra water-repellent films by microwave plasma-enhanced CVD, Thin Solid Films 1997;303(1/2):222–225

69 M.A.Petrunin, A.P Nazarov and Y.N. Mikhailovski, Formation mechanism and anticorrosive properties of thin siloxane films on metal surfaces. Journal of Electrochemical Society 1996;143:251–257
70 T.M. Mayer, M.P. de Boer, N.D. Shinn, P.J. Clews, T.A. Michalske, Chemical vapor deposition of fluoroalkylsilane monolayer films for adhesion control in microelectromechanical systems Journal of Vacuum Science & Technology B 2000;18:2433–2440
71 M.K.Chaudhury, Self-assembled monolayers on polymer surfaces, Biosensors and Bioelectronics 1995;10(9/10):785–788
72 T.G. Vargo, J.A. Gardella Jr, J.M. Calvert, M.S. Chen., Adhesive electroless metalization of fluoropolymeric substrates. Science 1993;262:1711-1712
73 E.P.J.M Everaert, H.C. van der Mei, H.J. Busscher, Adhesion of yeasts and bacteria to fluoro-alkylsiloxane layers chemisorbed on silicone rubber, Colloids and Surfaces B: Biointerfaces 1998:10;179– 190
74 C. Price, M.G.J. Waters, D.W. Williams, M.A.O. Lewis, D. Stickler, Surface modification of an experimental silicone rubber aimed at reducing initial candidal adhesion, Journal of Biomedical Materials Research 2002;63:122–128
75 T. Cao, H. Tang, X. Liang, A. Wang, G. W. Auner, S. O. Salley, K.Y. Simon Ng, E. coli to Surface Modified Silicone Using Atomic Force Microscopy, Biotechnology and Bioengineering 2006;94(1):167-176
76 Y. Xiu**,** Dennis W. Hess and C.P. Wong, UV and thermally stable superhydrophobic coatings from sol–gel processing, Journal of Colloid and Interface Science 2008;326:465–470
77 A.Wang, X. Liang, J. P. McAllister II, J. Li, K. Brabant, C. Black, P. Finlayson, T. Cao, H. Tang, S. O. Salley, G. W. Auner and K.Y. Simon Ng, Stability of and inflammatory response to silicon coated with a fluoroalkyl self-assembled monolayer in the central nervous system, Journal of Biomedical Materials Research Part A 2007;81A(2):363-372
78 D.A. Stenger, J.J. Hickman, K.E. Bateman, K.S. Ravenscroft, W. Ma, J.J. Pancrazio, Microlithographic determination of axonal: dendritic polarity in cultured hippocampal neurons. Journal of Neuroscience Methods 1998;82:167–173
79 D. Pavithra and M. Doble, Biofilm formation, bacterial adhesion and host response on polymeric implants—issues and prevention, Biomedical Materials 2008;3
80 E. Eisenbarth, D Velten, M. Muller, R Thull and J. Breme, Nanostructured niobiuym oxide coatings influence osteblast adhesion, Journal of Biomedical Materials Research Part A, Published online 20 June 2006, DOI 10.1002/jbm-a
81 S. Kato, T. Akagi, K. Sugimura, A Kishida and M Akashi, Evaluation of biological responses to polymeric biomaterials by RT-PCR analysis IV study of c-myc, c-fos and p53 m RNA expression, Biomaterials 2000;21:521–527
82 M.A.B Kruft, F.H.Van der Veen and L.H. Koole, In vivo tissue compatibility of two radio-opaque polymeric biomaterials, Biomaterials 1997;18:31–36

83 J. Wilson, R. E. Clegg, D. I. Leavesley and M. J. Pearcy, Mediation of Biomaterial–Cell Interactions by Adsorbed Proteins: A Review, Cameron Tissue Engineering 2005;11(1-2):1-18
84 N. J. Sniadecki, R. A. Desai, S. A. Ruiz, and C. S. Chen, Nanotechnology for Cell–Substrate Interactions, Annals of Biomedical Engineering 2006;34(1):59-74
85 Y. Koc, A. J. de Mello, G. McHale, M. I. Newton, P. Roacha and N. J. Shirtcliffe, Nano-scale superhydrophobicity: suppression of protein adsorption and promotion of flow-induced detachment, Lab Chip 2008;8,582–586
86 Y. Wu, F. Simonovsky, B. Ratner and T. Horbett, The role of adsorbed fibrinogen in platelet adhesion to polyurethane surfaces: A comparison of surface hydrophobicity, protein adsorption, monoclonal antibody binding, and platelet adhesion, Journal of Biomedical Materials Research A 2005;74(4):722–738
87 J.L. Brash., and T.A. Horbett, Proteins at interfaces: An overview. In: T.A. Horbett, and J.L. Brash, eds. Proteins at Interfaces II: Fundamentals and Applications, Washington, D.C.: American Chemical Society 1995; 2:1–23
88 J.L.Brash, Mechanism of adsorption of proteins to solid surfaces and its relationship to blood compatibility. In: M. Szycher ed. Biocompatible Polymers, Metals, and Composites. Technomic publishing company 1983;35–52
89 W. Norde and C.A. Haynes, Reversibility and the mechanism of protein adsorption. In: T.A. Horbett, and J.L. Brash, eds. Proteins at Interfaces II: Fundamentals and Applications. Washington, D.C.: American Chemical Society 1995;26–40
90 T.A. Horbett, Proteins: Structure, properties, and adsorption to surfaces. In: B.D. Ratner, A.S. Hoffman, F.J. Schoen and J.E. Lemons, eds. Biomaterials Science, Academic Press 1996;133–141.
91 C.A. Haynes and W. Norde, Globular proteins at solid/liquid interfaces, Colloids Surfaces B. Biointerfaces 1994;2(6):517-566
92 C.F. Wertzand and M.M. Santore, Adsorption and relaxation kinetics of albumin and fibrinogen on hydrophobic surfaces: Single-species and competitive behavior, Langmuir 1999;15(26):8884-8894
93 D.J. Fabrizius-Homan and S.L. Cooper, Competitive adsorption of vitronectin with albumin, fibrinogen, and fibronectin on polymeric biomaterials, Journal of Biomedical Materials Research 1991;25:953-971
94 S.M. Slack and T.A. Horbett, Physicochemical and biochemical aspects of fibrinogen adsorption from plasma and binary protein solutions onto polyethylene and glass, Journal of Colloid Interface Science 1988;124:535-551
95 Y.Arima and H. Iwata, Effect of wettability and surface functional groups on protein adsorption and cell adhesion using well-defined mixed self-assembled monolayers, Biomaterials 2007;28(20):3074-3082
96 L. Vroman and A.L. Adams, Adsorption of proteins out of plasma and solutions in narrow spaces, Journal of Colloid Interface Science 1986;111:391-402

97 S.M. Slack and T.A. Horbett, The Vroman effect: A critical review. In: T.A. Horbett, and J.L. Brash, eds. Proteins at Interfaces II: Fundamentals and Applications. Washington, D.C.: American Chemical Society 1995:112–128
98 R.J. Green, M.C. Davies, C.J. Roberts and S.J.B. Tendler, Competitive protein adsorption as observed by surface plasmon resonance. Biomaterials 1999;20:385-391
99 F. Grinnell, Focal adhesion sites and the removal of substratum- bound fibronectin, Journal of Cell Biology 1986;103:2697-2706
100 M.T. Khorasani and H. Mirzadeh, BHK cells behavior on laser treated polydimethylsiloxane surface, Colloids and Surfaces B: Biointerfaces 2004;35:67–71
101 T. Okano, N. Yamada, M. Ckuhora, H. Sakai, Y. Sakurai, Mechanism of cell detachment from temperature-modulated, hydrophilic-hydrophobic polymer surfaces Biomaterials 1995;16:297-303
102 J. Folkman and A. Moscona, Role of cell shape in growth control, Nature 1978;273, 345-349
103 A. Ben-Ze'ev, S.R. Farmer and S. Penman, Protein synthesis requires cell-surface contact while nuclear events respond to cell shape in anchorage-dependent fibroblasts, Cell 1980;21:365-372
104 R. Singhvi, A. Kumar, G.P. Lopez, G.N. Stephanopoulos, D.I. Wang, G.M. Whitesides and D.E. Ingber, Engineering cell shape and function, Science 1994;264:696-698
105 J. Takebe, C.M. Champagne, S. Offenbacher, K. Ishibashi and L.F. Cooper, Titanium surface topography alters cell shape and modulates bone morphogenetic protein 2 expression in the J774A.1 macrophage cell line, Journal of Biomedical Materials Research 2003;64A(2),207-216
106 R. McBeath, D.M. Pirone, C.M. Nelson, K. Bhadriraju and C.S. Chen, Cell shape, cytoskeletal tension, and RhoA regulate stem cell lineage commitment, Developmental Cell 2004;6:483-495
107 F. Grinnell and M.K. Feld, Fibronectin adsorption on hydrophilic and hydrophobic surfaces detected by antibody binding and analyzed during cell adhesion in serum-containing medium, Journal of Biological Chemistry 1982;257:4888-4893
108 Hayman, E.G., Pierschbacher, M.D., Suzuki, S., and Ruoslahti, E. Vitronectin—a major cell attachment-promoting protein in fetal bovine serum, Experimental Cell Research 1985;160:245-258
109 B. Alberts, A. Johnson, J. Lewis, M. Raff, K. Roberts, and P. Walter, Molecular Biology of the Cell. New York, NY: Garland Science 2002
110 K. Burridge and M. Chrzanowska-Wodnicka, Focal adhesions, contractility, and signaling, Annual Review of Cell and Developmental Biology 1996;12:463–518
111 F.G. Giancotti, A structural view of integrin activation and signaling, Developmental Cell 2003;4:149-151
112 D.D. Schlaepfer, C.R. Hauck and D.J. Sieg, Signaling through focal adhesion kinase. Progress in Biophysics and Molecular Biology 1999;71:435–478

113 K.A. DeMali, K. Wennerberg and K. Burridge, Integrin signaling to the actin cytoskeleton, Current Opinion in Cell Biology 2003;15:572–582.
114 B. Geiger, A. Bershadsky, R. Pankov and K. M. Yamada, Transmembrane extracellular matrix–cytoskeleton crosstalk, Nature Reviews Molecular Cell Biology 2001; 2:793–805
115 G. Schneider and K. Burridge, Formation of focal adhesions by osteoblasts adhering to different substrata, Experimental Cell Research 1994;214:264-269
116 I.I. Singer, S. Scott, D.W. Kawka, D.M. Kazazis, J. Gailit and E. Ruoslahti, Cell surface distribution of fibronectin and vitronectin receptors depends on substrate composition and extracellular matrix accumulation, Journal of Cell Biology 1988;106:2171-2182
117 M. Hormia and M. Könönen, Immunolocalization of fibronectin and vitronectin receptors in human gingival fibroblasts spreading on titanium surfaces, Journal of Periodontal Research 1994;29:146-152
118 M.C. Siebers, P.J. ter Brugge, X.F. Walboomers and J.A. Jansen, Integrins as linker proteins between osteoblasts and bone replacing materials: A critical review, Biomaterials 2005;26:137-146
119 J. Clover, R.A. Dodds and M. Gowen, Integrin subunit expression by human osteoblasts and osteoclasts in situ and in culture, Journal of Cell Science 1992;103:267-271
120 A. Diener, B. Nebe, F. Luthen, P. Becker, U. Beck, H. G. Neumann and J. Rychly, Control of focal adhesion dynamics by material surface characteristics, Biomaterials 2005; 26:383-392
121 S. L. Goodman, P.A. Sims and R.M. Albrecht, Three-dimensional extracellular matrix textured biomaterials. Biomaterials 1996;17(21):2087-2095.
122 M. Könönen, M. Hormia, J. Kivilahti, J. Hautaniemi and I. Thesleff, Effect of surface processing on the attachment, orientation and proliferation of human gingival fibroblasts on titanium, Journal of Biomedical Materials Research 1992;26:1325-1341
123 T.G. van Kooten and A.F. von Recum, Cell adhesion to textured silicone surfaces: the infuence of time of adhesion and texture on focal contact and fibronectin formation, Tissue Engineering 1999;5:223–240
124 X.F. Walboomers, J.A. Jansen, Cell and tissue behavior on micro-grooved surfaces, Odontology 2001;89:2–11
125 C.D.W. Wilkinso, M. Riehle, M. Wood, J.Gallagher and A.S.G. Curtis, The use of materials patterned on a nano- and micrometric scale in cellular engineering, Materials Science & Engineering: C 2002;19:263–269
126 M. Arnold, E.A. Cavalcanti-Adam, P. Glass, J. Blummel, W. Eck, M. Kantlehner, H. Kessler and J.P. Spatz, Activation of integrin function by nanopatterned adhesive interfaces, ChemPhysChem 2004;5:383–388
127 M. L. Carman, T.G. Estes, A. W. Feinberg, J. F. Schumacher, W. Wilkerson, L. H. Wilson, M. E. Callow, J. A. Callow and A. B. Brennan, Engineered antifouling microtopographies – correlating wettability with cell attachment, Biofouling 2006;22(1):11–21

128 C. de Vasconcelos, P. Bezerril, T. Dantas,M. Pereira and J. Fonseca, Adsorption of Bovine Serum Albumin on Template-Polymerized Chitosan/Poly(methacrylic acid) Complexes, Langmuir 2007;23(14):7687–7694
129 M. Lampin, R. Warocquier-Clerout, C. Legris, M. Degrange and M.F. Sigot-Luizard, Correlation between substratum roughness and wettability, cell adhesion and cell migration, Journal of Biomedical Materials Research 1997;36:99-108
130 F. Chen, C.N. Lee and S.H. Teoh, Nanofibrous modification on ultra-thin poly(-caprolactone) membrane via electrospinning, Materials Science & Engineering: C 2007;27:325-332
131 J.Y. Lim, J.C. Hansen, C.A. Siedlecki, R.W. Hengstebeck, J. Cheng, N. Winograd and H.J. Donahue, Osteoblast adhesion on poly(L-lactic acid)/polystyrene demixed thin film blends: Effect of nanotopography, surface chemistry and wettability, Biomacromolecules 2005;6:3319-3327
132 C. Xu, F.Yang, S. Wang and S.Ramakrishna, In vitro study of human vascular endothelial cell function on materials with various surface roughness, Journal of Biomedical Materials Research A 2004;71:154-161
133 G.R. Owen, J. Jackson, B. Chehroudi, H. Burt and D.M. Brunette, A PLGA membrane controlling cell behaviour for promoting tissue regeneration, Biomaterials 2005;26:7447-7456
134 H.L. Khor, Y. Kuan, H. Kukula, K. Tamada, W. Knoll, M. Moeller and D.W. Hutmacher, Response of cells on surface-induced nanopatterns: Fibroblasts and mesenchymal progenitor cells, Biomacromolecules 2007;8:1530-1540
135 A. Curtis and C. Wilkinson, Topographical control of cells, Biomaterials 1997;18(24):1573−1583
136 B. Wojciak-Stothard, A. Curtis, W. Monaghan, K. MacDonald and C. Wilkinson, Guidance and activation of murine macrophages by nanometric scale topography, Experimental Cell Research 1996;223(2):426-435
137 A. Curtis and C. Wilkinson, Nanotechniques and approaches in biotechnology, Trends in Biotechnology 2001;19:97–101
138 M.J. Dalby, M.O. Riehle, D.S. Sutherland, H. Agheli and A. S. G. Curtis, Fibroblast response to a controlled nanoenvironment produced by colloidal lithography, Journal of Biomedical Materials Research, Part A 2004;69A(2):314-322
139 E.A. Cavalcanti-Adam, A. Micoulet, J. Blummel, J. Auernheimer, H. Kessler and J.P. Spatz, Lateral spacing of integrin ligands influences cell spreading and focal adhesion assembly, European Journal of Cell Biology 2006;85(3-4):219-224
140 G. Mendonça, D. B.S. Mendonça, F. J.L. Aragao and L. F. Cooper, Advancing dental implant surface technology – From micron to nanotopography, Biomaterials 2008;29:3822–3835
141 E.A.Vogler, Structure and reactivity of water at biomaterial surfaces, Advanced Colloid Interface Science 1998;74:69-117
142 W. Norde, Adsorption of proteins from solution at the solid–liquid interface, Advanced Colloid Interface Science 1986;25:267-340

143 H. Worch, Special thin organic coatings. In: J.A. Helsen and H.J. Breme, eds. Metals as Biomaterials. Chichester: John Wiley & Sons 1998:177–196
144 W. Norde, and C.E. Giacomelli, BSA structural changes during homomolecular exchange between the adsorbed and the dissolved states, Journal of Biotechnology 2000;79:259-268
145 W. Norde, Driving forces for protein adsorption at solid surfaces. In: M. Malmsten, ed. Biopolymers at Interfaces, New York: Marcel Dekker 1998:27–54
146 D. Hanein, B. Geiger and L. Addadi, Fibronectin adsorptionto surfaces of hydrated crystals: An analysis of the importance of bound water in protein substrate interactions. Langmuir 1993;9:1058-1065
147 U. Jönsson, B. Ivarsson, I. Lundström and L. Berghem, Adsorption behavior of fibronectin on well characterized silica surfaces, Journal of Colloid Interface Science 1982;90:148
148 D.R. Absolom, W. Zingg and A.W. Neumann, Protein adsorption to polymer particles: Role of surface properties, Journal of Biomedical Materials Research 1987;21:161-171
149 D.E. MacDonald, N. Deo, B. Markovic, M. Stranick and P. Somasundaran, Adsorption and dissolution behavior of human plasma fibronectin on thermally and chemically modified titanium dioxide particles, Biomaterials 2002;23:1269-1279
150 H.B. Elwing, L. Li, A.R. Askendal, G.S. Nimeri and J.L. Brash, Protein displacement phenomena in blood plasma and serum studied by the wettability gradient method and the lens-on-surface method. In: T.A. Horbett and J.L. Brash, eds. Proteins at Interfaces II: Fundamentals and Applications. Washington, D.C.: American Chemical Society 1995:138–149.
151 S. Margel, E.A.Vogler, L. Firment, T. Watt, S. Haynie and D.Y. Sogah, Peptide, protein and cellular interactions with self-assembled monolayer model surfaces, Journal of Biomedical Materials Research 1993;27:1463-1476
152 E. M. Harnett, J. Alderman and T. Wood, The surface energy of various biomaterials coated with adhesion molecules used in cell culture, Colloids and Surfaces B: Biointerfaces 2007;55:90–97
153 Y. Tamada and Y. Ikada, Effect of preadsorbed proteins on cell adhesion to polymer surfaces, Journal of Colloid Interface Science 1993;155:334–339
154 J.H. Lee, G. Khang, J.W. Lee and H.B. Lee, Interaction of different types of cells on polymer surfaces with wettability gradient, Journal of Colloid Interface Science 1998;205:323–330
155 T.G. Ruardy, J.M. Schakenraad, H.C. van der Mei and H.J. Busscher, Adhesion and spreading of human skin fibroblasts on physicochemically characterized gradient surfaces, Journal of Biomedical Materials Research 1995;29:1415–1423
156 G.S. Senesi, E. D'Aloia, R. Gristina, P. Favia, R. d'Agostino, Surface characterization of plasma deposited nano-structured fluorocarbon coatings for promoting in vitro cell growth, Surface Science 2007;601:1019–1025

157 H. Zhang, R. Lamb and J. Lewis, Engineering nanoscale roughness on hydrophobic surface—preliminary assessment of fouling behavior, Science and Technology of Advanced Materials 2005;6:236–239
158 P. Roach, N. Shirtcliffe, D. Farrar and C. Perry, Quantification of Surface-Bound Proteins by Fluorometric Assay: Comparison with Quartz Crystal Microbalance and Amido Black Assay, Journal of Physical Chemistry B 2006;110(41):20572–20579
159 H.J. Busscher, I. Stokroos, J.G. Golverdingen and J.M. Schakenraad, Adhesion and Spreading of Human Fibroblasts on Superhydrophobic FEB-teflon, Cells and Materials 1991;1(3):243-249
160 Y.Q. Wang and J.Y. Cai, Enhanced cell affinity of poly(L-lactic acid) modified by base hydrolysis: Wettability and surface roughness at nanometer scale, Current Applied Physics 2007;7:108-111
161 S. Bauer, J. Park, K. von der Mark and P. Schmuki, Improved attachment of mesenchymal stem cells on super-hydrophobic TiO2 nanotubes, Acta Biomaterialia 2008;4:1576–1582
162 A.L. Sieminski and K.J. Gooch, Biomaterial-microvasculature interactions, Biomaterials 2000;21:2233-2241
163 M. T. Khorasani and H. Mirzadeh, Blood Compatibility of Modified PDMS Surfaces as Superhydrophobic and Superhydrophilic Materials, Journal of Applied Polymer Science 2004;91:2042–2047
164 R. Bahulekar, N. Tamura, S. Ito and M. Kodama, Platelet adhesion and complement activation studies on poly(*N*-alkyl mono and disubstituted) acrylamide derivatives, Biomaterials 1999;20:357-362
165 T. Matsuda and S. Ito, Surface coating of hydrophilic-hydrophobic block co-polymers on a poly(acrylonitrile) haemodialyser reduces platelet adhesion and its transmembrane stimulation, Biomaterials 1994;13:417-422
166 S. Hoffman, A. S.; Cohn, D.; Hanson, S. R.; Harker, L. A.; Horbett, T. A.; Ratner, B. D.; Reynolds, L. O. Radiat Phys Chem 1983, 22, 267.
167 T.Sun, H. Tan, D. Han, Q. Fu and L. Jiang, No Platelet Can Adhere—Largely Improved Blood Compatibility on Nanostructured Superhydrophobic Surfaces, Small 2005;1(10):959 – 963
168 G.J. Toes, K.W. van Muiswinkel, W. van Oeveren, A.J.H. Suurmeijer, W. Timens, I. Stokroos and J.J.A.M. van den Dungen, Superhydrophobic modification fails to improve the performance of small diameter expanded polytetrafluoroethylene vascular grafts, Biomaterials 2002;23(1):255–262
169 J.M. Schakenraad, I. Stokroos, H. Bartels and H.J. Busscher, Patency of small caliber, superhydrophobic ePTFE vascular grafts; a pilot study in the rabbit carotid artery, Cells and Materials 1992;2:193-199
170 J.M. Schierholz and J. Beuth, Implant infection: a haven for opportunistic bacterial, Journal of Hospital Infection 2001;49:87-93
171 R. A. Freitas Jr, Nanomedicine vol IIA Biocompatibility, Landes Bioscience 2003, ISBN: 978-1-57059-700-8

172 R M. Donlan and J.W. Costerton, Biofilm: survival mechanisms of clinically relevant microorganisms, Clinical Microbiology Review 2002;15:167–193
173 R.F. Padera, Infection in ventricular assist devices: the role of biofilm, Cardiovascular Pathology 2006;15:264–270
174 P. Tenke, M. Jackel and E. Nagy, Prevention and treatment of catheter associated infections: myth or reality? EAU Update Series 2004;2:106–115
175 N. Cerca, G.B. Pier, M. Vilanova, R. Oliveira and J. Azeredo, Quantitative analysis of adhesion and biofilm formation on hydrophilic and hydrophobic surfaces of clinical isolates of Staphylococcus epidermidis, Research in Microbiology 2005;156:506–514
176 M. Katsikogianni and Y.F. Missirlis, Concise review of mechanisms of bacterial adhesion to biomaterials and of techniques used in estimating bacteria—material interactions, European Cells and Materials 2004;8:37–57
177 R. Van Houdt and C.W. Michiels, Role of bacterial cell surface structures in Escherichia coli biofilm formation, Research in Microbiology 2005; 156:626–33
178 C.I. Locatelli, S. Kwitko and S. Amauri Braga, Conjunctival endogenous microbiota in patients submitted to cataract surgery, Brazilian Journal of Microbiology 2003;34:203–209
179 A.H. Hogt, J. Dankert, C.E. Hulstaert and J. Feijen, Cell surface characteristics of coagulase—negative Staphylococci and their adherence to fluorinated poly(ethylene propylene), Infect. Immun. 1986 294–301
180 K.K. Jefferson,What drives bacteria to produce a biofilm? FEMS Microbiology Letters 2004;236:163–73
181 E.M.Werner, B. Huang, M.A. Hamilton and P.S. Stewart, Hypothesis for the role of nutrient starvation in biofilm detachment, Applied Environmental Microbiology 2004;70:7418–7425
182 M.B. Olde Riekerink, G.H.M. Engbers, H.C. Van der Mei, H.J. Busscher and J. Feijen, Microbial adhesion onto superhydrophobic fluorinated low density poly(ethylene) films. In: Thesis: Structural and Chemical Modification of Polymer Surfaces by Gas Plasma Etching. pp 65-82 2001
183 A.Wang, X. Liang, J. P. McAllister II, J. Li, K. Brabant, C. Black, P. Finlayson, T. Cao, H. Tang, S. O. Salley, G. W. Auner and K.Y. Simon Ng, Stability of and inflammatory response to silicon coated with a fluoroalkyl self-assembled monolayer in the central nervous system, Journal of Biomedical Materials Research Part A 2007;81A(2):363-372
184 Y. Xiu, F. Xiao, D. W. Hess and C.P. Wong, Superhydrophobic optically transparent silica films formed with a eutectic liquid, Thin Solid Films 2009;517:1610–1615
185 J. Lincks, B.D. Boyan, C.R. Blanchard, C.H. Lohmann, Y. Liu, D.L. Cochran, D.D. Dean and Z. Schwartz, Response of MG63 osteoblast-like cells to titanium and titanium alloy is dependent on surface roughness and composition, Biomaterials 1998;19(22):2219-2232
186 G. Zhao, Effects of Surface Microstructure and Nanostructure on Osteoblast-like MG63 Cell Number, Differentiation and Local Factor Production, Masters thesis In Partial

Fulfillment Of the Requirements for the Degree Master of Engineering in Biomedical Engineering Georgia Institute of Technology, November 2003

187 M, C. Alley, D. A. Scudiero, A. Monks, M. L. Hursey, M. J. Czerwinski, D. L. Fine, B. J. Abbott, J. G. Mayo, R. H. Shoemaker and M. R. Boyd, Feasibility of Drug Screening with Panels of Human Tumor Cell Lines Using a Microculture Tetrazolium Assay, Cancer Research 1988;48:589-601